TiAM

kwartalnik naukowo-techniczny

TECHNOLOGIA I AUTOMATYZACJA MONTAŻU

ZESPOŁÓW • MASZYN • URZĄDZEŃ

Wydawca: Łukasiewicz – IMBIGS • Oficyna Wydawnicza Politechniki Rzeszowskiej • Patronat SIMP • Istnieje od 1993 r.

Open Access: www.tiam.prz.edu.pl • Zeszyt nr 3/2022 (117)

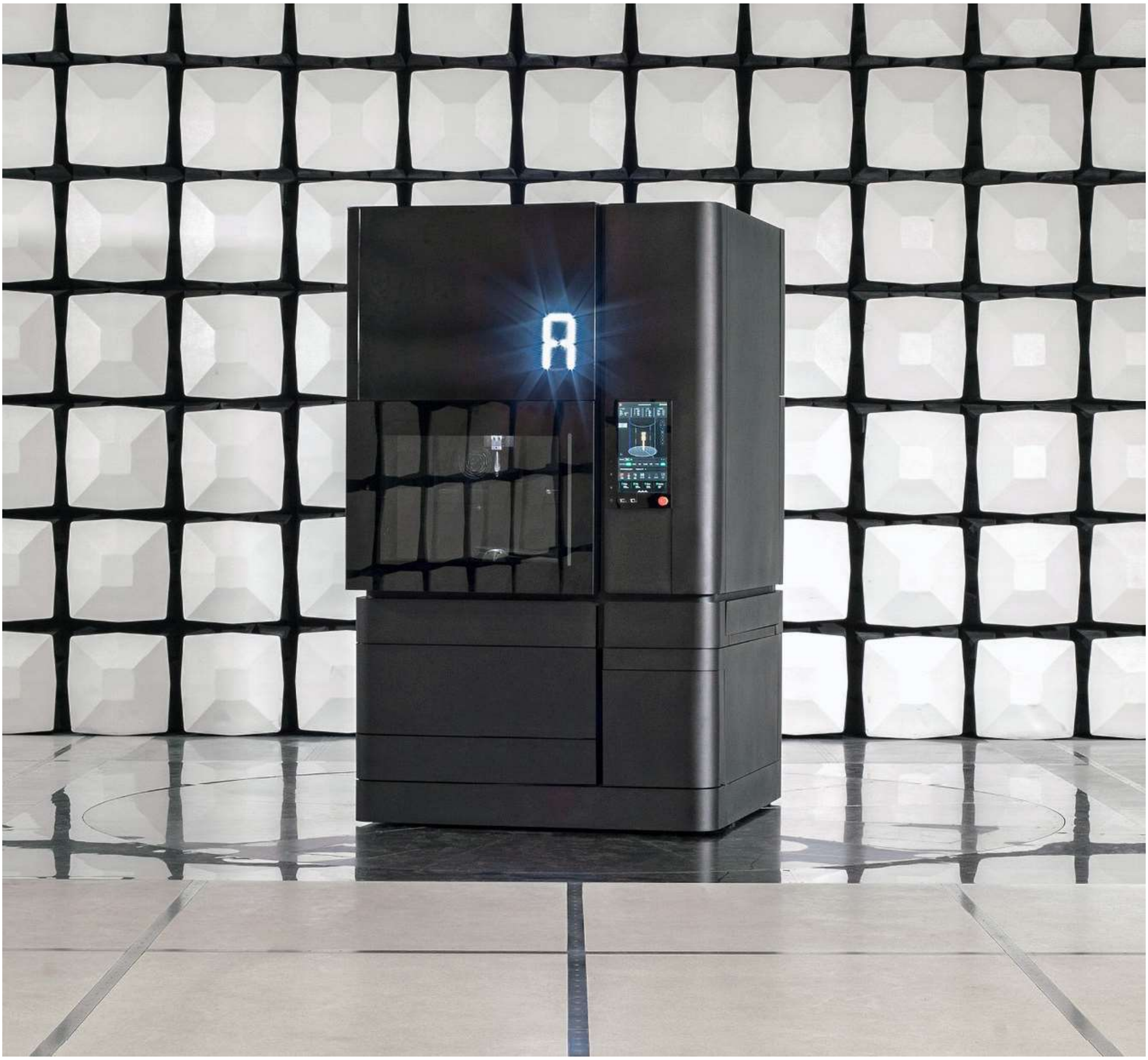

RZESZOW UNIVERSITY OF TECHNOLOGY

Łukasiewicz IMBiGS

TiAM kwartalnik naukowo-techniczny
TECHNOLOGIA I AUTOMATYZACJA MONTAŻU
ZESPOŁÓW • MASZYN • URZĄDZEŃ

ASSEMBLY TECHNIQUES AND TECHNOLOGIES

e-ISSN-2450-8217

ADRES REDAKCJI

Kwartalnik „Technologia i Automatyzacja Montażu" Al. Powstańców Warszawy 8, 35-959 Rzeszów, Poland, tel: +48 17 865 1452, fax.: +48 17 854 1184, e-mail: tiam@prz.edu.pl, www.tiam.prz.edu.pl

REKLAMA

Redakcja: tel:+48 17 865 1452, fax.: +48 17 865 1184, e-mail: tiam@prz.edu.pl

SKŁAD I ŁAMANIE

Oficyna Wydawnicza Politechniki Rzeszowskiej

WYDAWCA

Łukasiewicz IMBiGS

Sieć Badawcza Łukasiewicz
Instytut Mechanizacji Budownictwa i Górnictwa Skalnego
ul. Racjonalizacji 6/8, 02-673 Warszawa

RZESZOW UNIVERSITY OF TECHNOLOGY

Politechnika Rzeszowska,
al. Powstańców Warszawy 12, 35-959 Rzeszów

PATRONAT

Stowarzyszenie Inżynierów Mechaników i Techników Polskich
Za treść ogłoszeń i artykułów promocyjnych redakcja nie odpowiada
Wersja pierwotna: elektroniczna

WSKAZÓWKI DOTYCZĄCE PRZYGOTOWANIA ARTYKUŁÓW

- Artykuły przeznaczone do opublikowania w kwartalniku „Technologia i Automatyzacja Montażu" powinny mieć oryginalny i naukowo-techniczny charakter i być zgodne z problematyką czasopisma. Redakcja przyjmuje artykuły w jęz. polskim, jęz. angielskim i jęz. rosyjskim.
- Artykuł o maksymalnej objętości 5 stron A4 wraz z ilustracjami powinien być napisany czcionką Times Roman lub Arial 11 pkt, z interlinią 12 pkt. Formatowany tekst nie powinien mieć podziału na kolumny.
- Tytuł artykułu należy podać w jęz. polskim i jęz. angielskim. Tytuł nieprzekraczający 10 słów powinien odzwierciedlać istotne elementy treści artykułu.
- Struktura artykułów naukowo-technicznych prezentujących prace autora(ów) powinna być następująca: wstęp (wprowadzenie); metodyka (badań, analiz, pracy z podaniem ewentualnie materiałów, założeń itp.); wyniki (badań, analiz); omówienie wyników; wnioski; spis literatury.
- Podpisy pod ilustracjami oraz tytuły tablic należy podać w jęz. artykułu i jęz. angielskim.
- Ilustracje należy dołączyć również jako osobne pliki w formacie: .jpg, .tiff, z rozdzielczością co najmniej 300 dpi. Wszystkie zamieszczane ilustracje powinny być własnością autora(ów) lub należy podać źródło pochodzenia rysunków.
- Wzory matematyczne pisane w edytorze równań Microsoft Equation i powinny być oznaczane kolejnym numerem w nawiasie okrągłym. Wszystkie symbole powinny być objaśnione. Należy stosować jednostki układu SI.
- Spis literatury należy podać w kolejności cytowania w tekście, a odnośniki w tekściepo winny być ponumerowane cyframi arabskimi i umieszczone w nawiasach kwadratowych. W przypadku korzystania z Internetu należy podać adres strony i datę odczytu. Liczbę autocytowań należy ograniczyć do niezbędnych.
- Do artykułu należy dołączyć streszczenie w jęz. artykułu i jęz. angielskim, zawierające minimum 200-250 słów.
- Pod streszczeniem należy podać 3-6 słów kluczowych w jęz. artykułu i jęz. angielskim, zwracając uwagę, by nie były one powtórzeniem tytułu pracy.
- Po spisie literatury zaleca się podanie źródła finansowania pracy.
- Na końcu artykułu należy podać: imiona i nazwiska autorów, tytuły naukowe lub zawodowe, telefon, faks, e-mail, miejsce zatrudnienia wraz z adresem do korespondencji.

PROCEDURA RECENZOWANIA

Procedura recenzowania artykułów w czasopiśmie jest zgodna z zaleceniami Ministerstwa Naukii Szkolnictwa Wyższego zawartymi w opracowaniu „Dobre praktyki w procedurach recenzyjnych w nauce", Warszawa 2011.

Wszystkie artykuły naukowo-techniczne publikowane w kwartalniku „Technologia i Automatyzacja Montażu" są recenzowane.

Nadesłane artykuły są poddawane redakcyjnej ocenie formalnej i otrzymują numer redakcyjny, identyfikujący je na dalszych etapach procesu wydawniczego, a redakcja wysyła do autorów informację o przyjęciu artykułu i wysłaniu go do recenzentów. Do oceny każdej publikacji powołuje się co najmniej dwóch niezależnych recenzentów. Redakcja dobiera recenzentów rzetelnych i kompetentnych w danej dziedzinie. Nadesłane artykuły nie są nigdy wysyłane do recenzentów z tej samej placówki, z której pochodzi autor. Prace recenzentów są poufne i anonimowe. Recenzja musi mieć formę pisemną i kończyć się jednoznacznym wnioskiem o dopuszczeniu artykułu do publikacji w czasopiśmie lub jego odrzuceniu. W przypadku pracy w języku obcym, co najmniej jeden z recenzentów jest afiliowany w instytucji zagranicznej innej niż narodowość autora pracy. Autorzy są informowani o wynikach recenzji oraz otrzymują je do wglądu. W sytuacjach spornych redakcja powołuje dodatkowych recenzentów.

Lista recenzentów publikowana jest w ostatnim zeszycie każdego rocznika.

Kwartalnik „Technologia i Automatyzacja Montażu" ukazuje się w formie elektronicznej w otwartym dostępie (Open Access) i jest dostępny na www.tiam.prz.edu.pl

CONTENTS / W NUMERZE

Kwartalnik notowany na liście czasopism punktowanych Ministerstwa Edukacji i Nauki – 40 pkt.

TiAM kwartalnik naukowo-techniczny
TECHNOLOGIA I AUTOMATYZACJA MONTAŻU
ZESPOŁÓW • MASZYN • URZĄDZEŃ

Jan Godzimirski[1], Andrzej Komorek[2]

DOI: 10.7862/tiam.2022.3.1

IMPACT STRENGTH OF HYBRID JOINTS

UDARNOŚĆ POŁĄCZEŃ HYBRYDOWYCH

Abstract

Hybrid adhesive-mechanical joints compared to only adhesive or only mechanical joints are characterized by many advantages: greater stiffness, greater static strength, greater fatigue life, higher reliability, corrosion resistance. For these reasons, they are eagerly used in aviation structures. The aim of the research was to check the influence of hybridization on the impact toughness of connections. The static strength and the energy of dynamic destruction of lap joints loaded in shear by stretching or bending were compared: adhesive, riveted and hybrid joints. The tested hybrid joints were characterized by higher strength and dynamic destruction energy compared to adhesively bonded or riveted samples. The research also shows that the energy of dynamic failure increases if the failure of the joint is not complete and causes the connected elements to rotate around one rivet.

Keywords: hybrid adhesive-rivet joints, static strength, impact destruction energy

Streszczenie

Połączenia hybrydowe klejowo-mechaniczne w porównaniu do połączeń tylko adhezyjnych czy tylko mechanicznych charakteryzuje wiele zalet: większa sztywność, większa wytrzymałość statyczna, większa trwałość zmęczeniowa, wyższa niezawodność, odporność na korozję. Z tych względów chętnie są stosowane w konstrukcjach lotniczych. Celem prowadzonych badań było sprawdzenie wpływu hybrydyzacji na udarność połączeń. Porównano wytrzymałość statyczną oraz energię niszczenia dynamicznego połączeń zakładkowych obciążonych na ścinanie poprzez rozciąganie lub zginanie: klejowych, nitowych i hybrydowych. Badane połączenia hybrydowe cechowała większa wytrzymałość i energia niszczenia dynamicznego w porównaniu z próbkami klejonymi lub nitowanymi. Z badań wynika również, że energia niszczenia dynamicznego wzrasta, jeśli zniszczenie połączenia nie jest całkowite i powoduje obrót łączonych elementów wokół jednego nitu.

Słowa kluczowe: połączenia hybrydowe klejowo-nitowe, wytrzymałość statyczna, energia niszczenia udarowego

1. Introduction

The hybrid joint can be a combination of a mechanical joint and an adhesive joint. The appropriate configuration of the hybrid connection allows to eliminate the shortcomings of these connection techniques, and thus to obtain a structural node with better strength and operational properties [3, 6, 8, 12, 13, 14, 15, 17]. Many types of hybrid connections have been used in aviation structures: weld-adhesive, rivet-adhesive, clinch-adhesive and screw-adhesive [1, 2, 7]. This is due to the fact that the use of mechanical fasteners causes a high concentration of stresses around the mounting holes or welds [9], and this negative phenomenon can be partially limited by using an adhesive bond in the structural node alongside the mechanical connection.

The combination of mechanical and adhesive joints was also used to relieve the adhesive joint and reduce the negative impact of stress concentration at the edges of the joints. The right places for fasteners installation seem to be the ends of the adhesive joints, where the phenomenon of stress accumulation, especially normal stresses perpendicular to the adhesive joint, causes peeling.

The double system of connections is also a way of securing in a situation where one of the connections - most often the adhesive connection [18] - becomes damaged. Due to the assembly technology, the use of mechanical fasteners usually facilitates the assembly of the adhesively bonded elements and replaces the troublesome process of generating pressures during the hardening of the adhesive joint.

[1] prof. dr. hab. inż. Jan Godzimirski Department of Mechatronics, Armament and Aviation, Military University of Technology, ORCID: 0000-0003-1595-2057.
[2] dr hab. inż. Andrzej Komorek prof. LAW, Department of Aviation, Polish Air Force University, ORCID: 0000-0002-2293-714X.

Hybrid joints compared to only adhesive or only mechanical joints are characterized by [1, 4, 10, 16]: greater stiffness, greater static strength, greater fatigue life, higher reliability, corrosion resistance. Such connections are eagerly used for joining composites [5, 11].

The aim of the research was to check whether the impact strength can also be increased by the hybridization of riveted and adhesive joints.

2. Research methodology

The tests were carried out on two types of lap joints, loaded in shear by tension and by bending. The first type of samples was made by joining plates with dimensions of 70 x 20 x 2 mm made of AW 2024T3 aluminum alloy (material commonly used in aircraft construction) with an overlap of 24.5 mm by the method of adhesive bonding, riveting, adhesive bonding and riveting (Fig. 1).

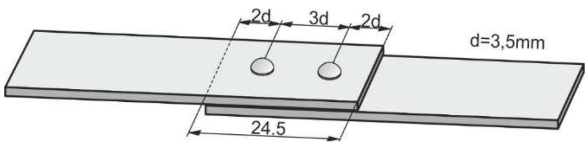

Fig. 1. The spacing of rivets in the lap sample, loaded by tension

Epidian 57/Z1 adhesive was used and two rivets with a diameter of 3.5 mm with countersunk heads made of PA24 alloy. The adhesively bonded surfaces of the samples were sandblasted with aluminum oxide and degreased with extraction gasoline. The adhesive layers were hardened in two stages: 12 hours at the ambient temperature and 5 hours at the temperature of 80ºC. The dimensions of the samples were determined by the capabilities of the Julietta impact hammer adapted to such tests. The samples were loaded in shear by stretching the joined elements. Three batches of samples (adhesively bonded, riveted and hybrid) were prepared, each of 15 pieces, 5 of which were intended for static strength tests, and 10 for dynamic tests. The static tests were carried out on the Hung Ta HT-2402 testing machine with a speed of 2 mm/min. In the impact tests, the holder mounted on the sample (Fig. 2) was hit with the energy of 25 J at a speed of 3.83 m/s.

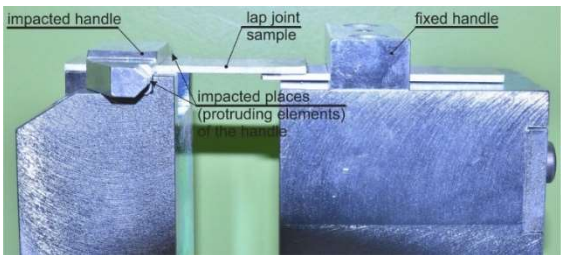

Fig. 2. Method of fixing lap specimens in impact tests

The second type of samples was made by joining steel plates with dimensions of 45 x 12 x 5 mm with an overlap of 25 mm by the method of adhesive bonded, riveting, adhesive bonded and riveting. Steel is a material used in the construction of motor vehicles for which impact strength is an important feature due to the possibility of participating in a collision. Loctite EA 9464 adhesive was used, two rivets with a diameter of 3.5 mm with ball heads made of PA24 alloy, spaced 7-11-7 mm. The adhesively bonded surfaces were roughened with abrasive cloth of granulation 80 and washed with gasoline. The adhesive layers were hardened for 5 days at ambient temperature. The samples were loaded on the wall by symmetrically bending them with double-sided support. The load was applied symmetrically to the surface perpendicular to the edge of the adhesive joint (Fig. 3).

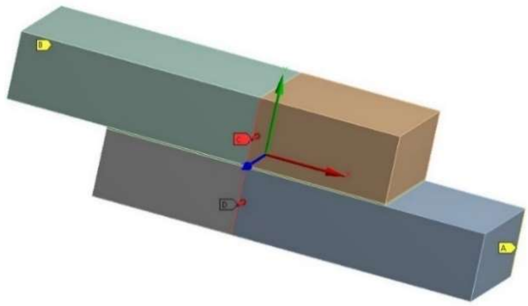

Fig. 3. Model of loading of lap samples by bending

There were prepared 3 batches of samples (adhesively bonded, riveted and hybrid) with the number of 10 pieces, of which 5 were intended for static strength tests, and 5 for dynamic tests. The static bending strength of the samples was determined by pressing them in a special device (Fig. 4) in the Hung Ta HT-2402 testing machine at a speed of 2 mm/min with the supports spacing of 40 mm. Impact tests were performed on a SW-5 impact hammer with a speed of 3.8 m/s, hitting with an energy of 50 J

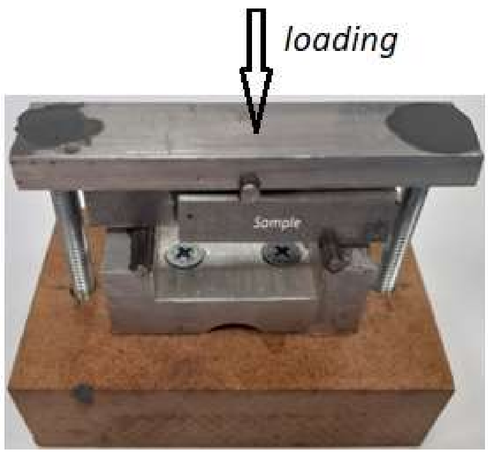

Fig. 4. The sample mounted in the device for testing the static strength by bending

3. Tests results

The lap joints loaded by tension

The results of the static strength tests are presented in Table 1 and Fig. 5 (the results in the tables are given with the confidence intervals calculated for the significance level of 95%).

Table 1. Results of the static strength tests

Joint	Adhesive	Riveted	Hybrid
Destructive force [N]	3593 ± 539	4604 ± 326	5668 ± 684
Average shear stress [MPa]	7.33 ± 1.10	9.40 ± 0.67	11.57 ± 1.40

The shear strength of the rivets was calculated:

$$R_t = \frac{F}{n\frac{\pi d^2}{4}} = \frac{4604}{2\frac{\pi 3{,}5^2}{4}} = 239\ \text{MPa}$$

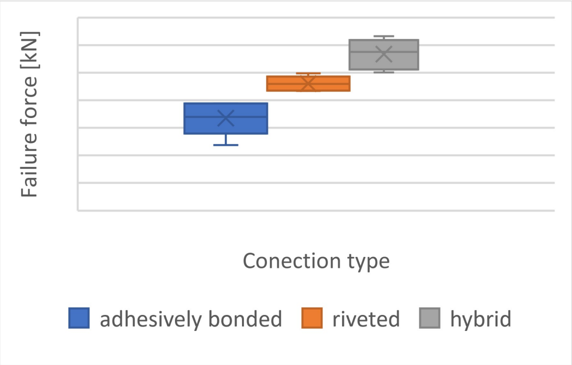

Fig. 5. Comparison of the resistance of different types of joints of lap specimens loaded by tension (X - median, mustache - maximum and minimum value, box - range 50% of the results (difference between the third and first quartile))

The strength of the tested joints differed significantly. The strength of the hybrid joints was the highest, but lower than the sum of the strength of the component connections, which is normal for this type of connection.

The dynamic test results conducted on the Julietta pendulum hammer with an energy of 25 J and a speed of 3.83 m/s are listed in Table 2 and in Fig. 6.

Table 2. Impact test results

Joint	Adhesive	Riveted	Hybrid
Destructive energy [J]	2.61±0.26	6.45±0.72	12.01±1.25
Average impact strength [kJ/m^2]	5.33±0.53	13.16±1.47	24.51±2.55

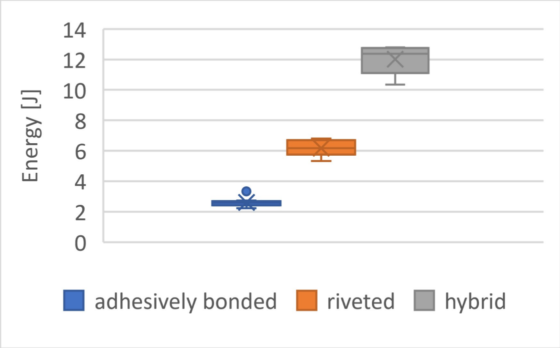

Fig. 6. Comparison of the failure energy of different types of tension lap joints

The destruction energy of hybrid samples turned out to be higher than the sum of the destruction energy of glued and riveted samples.

The lap joints loaded by bending

The results of the static strength tests of bended lap specimens are presented in Table 3 and Fig. 7.

Table 3. Results of the static strength tests

Joint	Adhesive	Riveted	Hybrid
Destructive force [N]	5347±481	3504±467	6662±593
Average shear stress [MPa]	17.82±1.60	11.68±1.55	22.2±21.98

The shearing force of one rivet can be calculated from the formula:

$$F_1 = \frac{F}{4}\left(1 + \frac{l}{2a}\right)$$

where: F - force destroying the connection, l - support spacing, a - rivet spacing.

The mean force calculated from this relationship has the value of 2469 N. It follows that the shear strength of the rivets used in the tests was:

$$R_t = \frac{F}{n\frac{\pi d^2}{4}} = \frac{2469}{1\frac{\pi 3{,}5^2}{4}} = 257\ \text{MPa}$$

The static strength of the adhesively bonded samples loaded in shear by bending was much higher than that of the tensile lap samples, despite the fact that the overlap samples were characterized by a larger area of the adhesive layer. The shear strength of the tested adhesives does not differ significantly, therefore the reason for the higher strength of the bended samples seems to be a lower share of normal stresses in the effort of the adhesive layers of joints loaded by bending and a much higher stiffness of the joined elements.

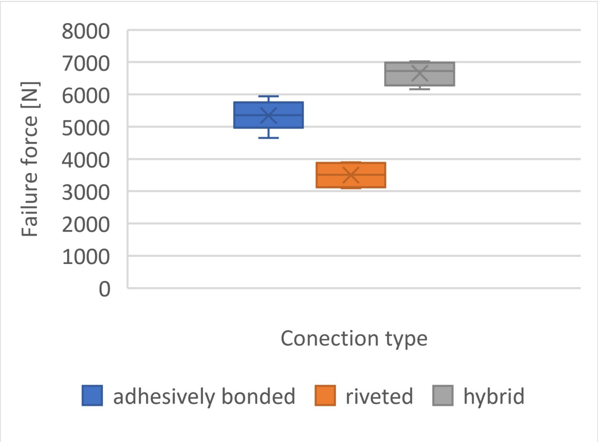

Fig. 7. Comparison of the resistance of different types of joints of lap specimens loaded in shear by bending

The results of the impact tests of the lap specimens loaded by bending are presented in Table 4 and Fig. 8.

Table 4. Impact test results

Joint	Adhesive	Riveted	Hybrid
Destructive energy [J]	3.78±0.49	8.8± 1.17	11.05±0.73
Average impact strength [kJ/m^2]	12.60±1.63	29.33±3.90	36.83±2.43

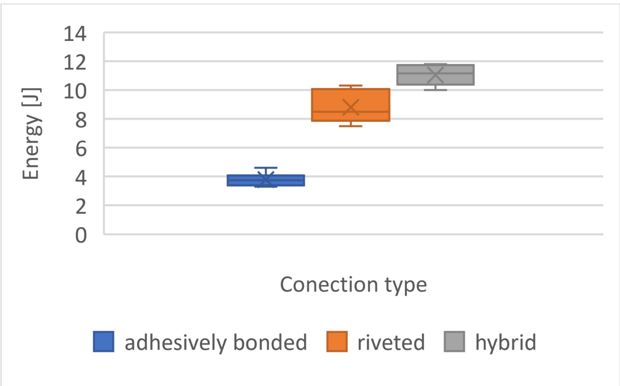

Fig. 8. Comparison of the failure energy of different types of joints of lap specimens loaded by bending

The riveted samples loaded by bending were characterized by a lower static strength compared to the lap samples, which is related to the adopted method of their loading, but the destruction energy was higher than that of the lap samples, despite the fact that in the case of tensile lap samples, two rivets were damaged, and in the case of bent samples, only one (Fig. 9). Therefore, it should be assumed that the rotation of the joined elements along the axis of the undamaged rivet consumed a significant part of the energy. Consequently, the impact strength of riveted and hybrid bend specimens that have undergone such failure is also overestimated. This is evidenced by the fact that four hybrid samples loaded by bending (which were not taken into account in the analysis of the results) were destroyed by cutting both rivets (Fig. 9), and their average failure energy of 7.05 J was lower than the destruction energy of hybrid samples in which only one rivet was damaged. It would also show that the adhesive causes a more even load of the mechanical connectors, which resulted in their simultaneous destruction.

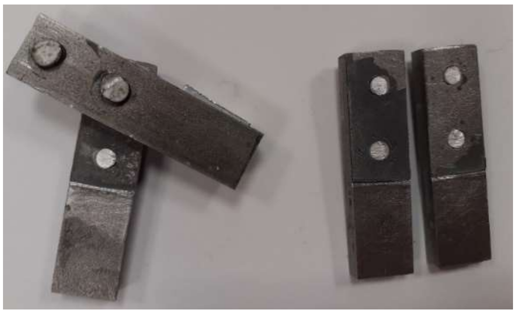

Fig. 9. Two methods of destroying hybrid lap joints of bended samples

The obtained results are difficult to relate to the literature data, as they were carried out on original, non-standardized samples. In addition, the literature data related to impact strength mainly concern combinations of different materials, which combinations are called hybrid, and not different duplicate joint systems.

4. Numerical analysis of samples loaded by bending

Numerical calculations of the statically loaded bended adhesive, riveted and hybrid joints were performed using the ANSYS system. Fig. 10 shows the hybrid connection load model and the mesh of elements. All analyzed joints were first loaded with the same force of 2000 N, because their purpose was mainly to estimate to what extent the adhesive joint would relieve the mechanical joints in a hybrid joint. The calculations were performed assuming linear properties of the adhesive (E = 2 GPa), joined steel elements (E = 200 GPa) and rivets (E = 72 GPa).

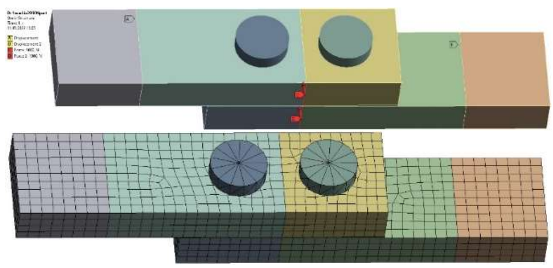

Fig. 10. The way of loading the hybrid connection and the mesh of elements

Figure 11 shows the von Mises stress distribution in the adhesive layer of an adhesive joint loaded by bending with a force of 2000 N.

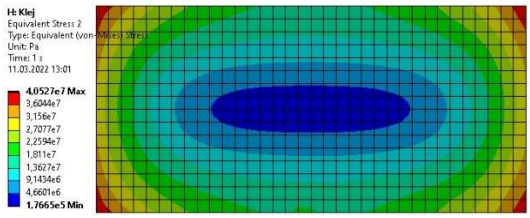

Fig. 11. Mises stress distribution in the adhesive layer of the joint loaded by bending with a force of 2000 N

Figure 12 shows the von Mises stress distribution in the shaft of the mechanical connector of a riveted joint loaded by bending with a force of 2000 N.

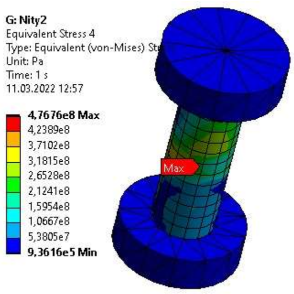

Fig. 12. Mises stress distribution in the shaft of the mechanical connector of a riveted joint, loaded by bending with a force of 2000 N

Fig. 13 shows the Mises stress distribution in the adhesive layer and in the shaft of the mechanical connector of hybrid joint, loaded by bending with a force of 2000 N.

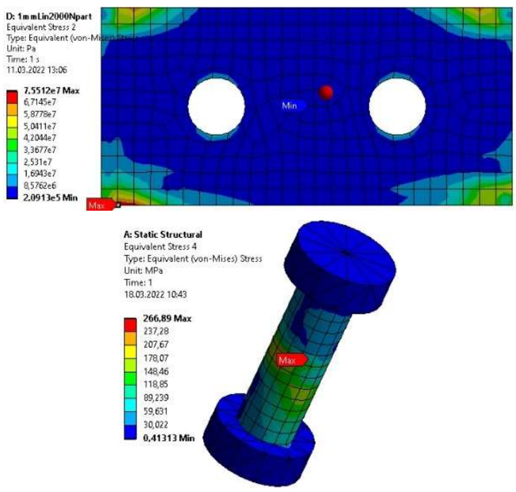

Fig. 13. Mises stress distribution in the adhesive layer and in the rivet body of a hybrid joint loaded by bending with a force of 2000 N

The performed calculations show that in the tested hybrid joint loaded by bending, the adhesive joint reduces the load of the rivet shafts more than twice. The use of rivets even increases the equivalent stresses in the adhesive joint but moves them away from the edge of the joint.

Since the calculated stresses in the adhesive joint exceeded the adhesive strength, additional calculations were made, taking into account the nonlinear properties of EA9464 adhesive (the mutilinaer isotropic hardening model - Fig. 14) and the aluminum alloy from which the rivets were made (bilinear isotropic hardening model - yield strength 330 MPa, strain hardening modulus 650 MPa).

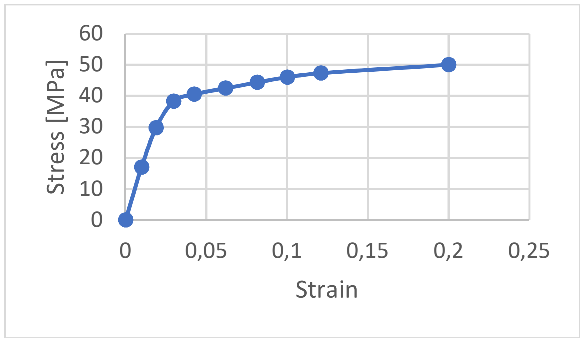

Fig. 14. The curve σ = σ (ε) of Loctite EA 9664 adhesive

In these calculations, the joints were loaded with experimentally determined destructive forces. The calculation results are shown in Figs. 15…17.

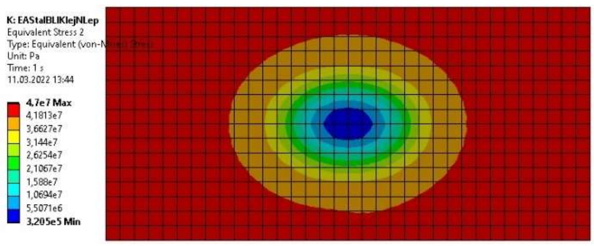

Fig. 15. Mises stress distribution in the adhesive layer of the joint loaded by bending with a force of 5347 N (nonlinear properties of the adhesive)

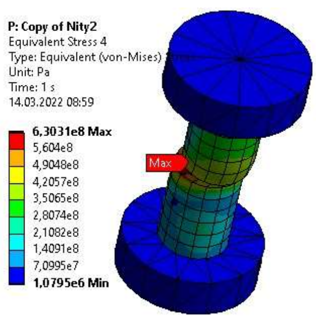

Fig. 16. Mises stress distribution in the shaft of a mechanical connector of a riveted joint loaded by bending with a force of 3504 N (nonlinear properties of aluminum alloy)

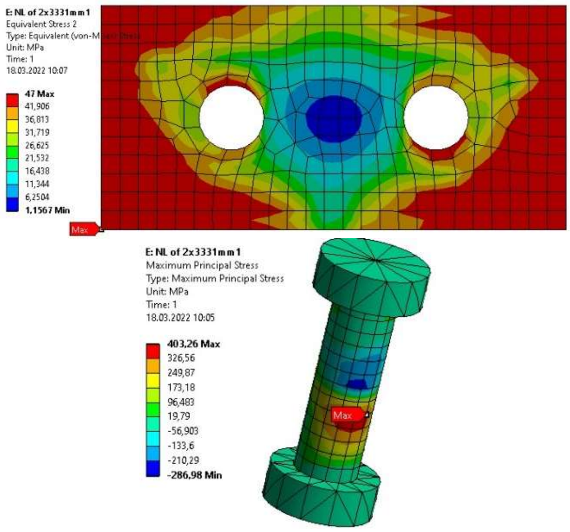

Fig. 17. Mises stress distribution in the adhesive layer and in the rivet body of a hybrid joint loaded by bending with a force of 6662 N (nonlinear properties of the adhesive and aluminum alloy)

Taking into account the non-linear properties of the adhesive resulted in a more uniform loading of the adhesive layer over a larger area. The calculated stresses in the rivet shafts of the riveted joint had values greater than the actual stresses of the alloy they are made of by about 17%, which may result from the too low value of the declared coefficient of friction (f = 0.1) between the joined elements. Taking into account the calculated values of destructive stresses of adhesive and rivet, it can be concluded that the analyzed hybrid joint the adhesive should be destroyed first, and then the rivets.

5. Conclusions

Hybrid joints are characterized by higher strength and impact strength compared to adhesively bonded or riveted ones.

The impact strength and energy of impact failure of the tested adhesively bonded, riveted and hybrid overlapping samples differed significantly. In the case of overlapping samples loaded by tensile stress, the impact strength of hybrid samples turned out to be higher than the sum of the impact strengths of riveted and adhesively bonded samples. In the case of bending samples, the impact strength of hybrid samples was close to the sum of the impact strengths of adhesively bonded and riveted samples.

It can be assumed that in the case of tensile lap samples, the adhesive layer strengthened the rivet joint, which was characterized by a higher load capacity than the adhesive joint. In the case of samples loaded by bending, it was the other way round, and in this case the rivets only slightly strengthened the adhesive joint.

Tensile lap samples seem to be more suitable for the tests of the impact strength of hybrid connections, because both mechanical connectors are always sheared when damaged.

Numerical analysis of adhesively bonded, riveted or hybrid joints loaded with destructive forces requires taking into account the nonlinear material properties of such joints.

Literature

1. Balawender T., Sadowski T.,Knieć M., *Technological problems and experimental investigation of hybrid: clinched – adhesively bonded joint,* Archives of Metallurgy and Materials, 2013, vol. 56, 439-446.
2. Bodjona K., Lessard L., *Load sharing in single lap bonded/bolted composite joints. Part II: Global sensitivity analysis.* Composite Structures 129 (2015) 276–283.
3. Chang P., Wang J., Wing Kong Chiu, Nabil M. Chowdhury, *Experimental and finite elements studies of bolted, bonded and hybrid step lap joints of thick carbon fibre/epoxy panels used in aircraft structures*, Composites Part B 100, (2016), 68-77.
4. Chowdhury N., Chiu W.K., Chang P., *Static and fatigue testing thin riveted, bonded and hybrid carbon fiber double lap joints used in aircraft structures*. Composite Structures 121 (2015), 315-323.
5. Chowdhury N.M., Chiu W.K., Wang J., Chang P., *Experimental and finite element studies of bolted, bonded and hybrid step lap joints of thin carbon fibre/epoxy panels used in aircraft structures,* Composite Structures Part B 85 (2016), 232-242.
6. Da Silva L.F.M., Pirondi A., Ochsner A., *Hybrid Adhesive Joints*, Springer, 2011.
7. Esmaeili F., Zehsaz M., Chakherlou T.N., *Investigation the effect of tightening torque on the fatigue strength of double lap simple bolted and hybrid (bolted–bonded) joints using volumetric method,* Materials and Design 63 (2014), 349-359.
8. Franco G.Di., Fratini L., Pasta A., *Analysis of the mechanical performance of hybrid (SPR/bonded) single-lap joints between CFRP panels and aluminum blanks,* International Journal of Adhesion & Adhesives 41 (2013), 24-32.
9. Fu M., Mallic P., *Fatigue of hybrid (adhesive/bolted) joints in SRIM composites.* International Journal of Adhesion & Adhesives 21 (2001), 145-159.
10. Gómez S., Onoro J., Pecharroman J., *A simple mechanical model of a structural hybrid adhesive/riveted single lap joint.* Internal Journal of Adhesion & Adhesives 27 (2006), 263-267.
11. Kelly G., *Load transfer in hybrid (bonded/bolted) composite single-lap joints*, Composite Structures 69 (2005), 35-43.
12. Matwijenko W.A., *Wpływ czynników konstrukcyjno--technologicznych na wytrzymałość zmęczeniową połączeń klejowo-nitowych.* Technologia i Automatyzacja Montażu 2/1994, 33-35.
13. Pitta S., Roure F., Crespo D., Rojas J., *An experimental and numerical study of repairs on composite substrates with composite and aluminium doublers using riveted,*

bonded and hybrid joints, Multidisciplinary Digital Publishing Institute, Materials 2019, vol. 12, issue 18, 2978.

14. Rośkowicz M., Gąsior J., *Load capacity and fatigue life of hybrid joints.* Technologia i Automatyzacja Montażu 2/2019, 30-33. 4.
15. Rośkowicz M., Godzimirski J., Gąsior J., Jasztal M., *Improvement of fatigue life of riveted joints in helicopter airframes*, Eksploatacja i Niezawodność – Maintenance and Reliability, vol. 23 (2021), issue 1.
16. Rośkowicz M., Godzimirski J., Komorek A., Gąsior J., Jasztal M., *Influence of the arrangement of mechanical fasteners on the static strength and fatigue life of hybrid joints,* Multidisciplinary Digital Publishing Institute, Materials 2020, vol. 13, issue 23, 5308.
17. Sadowski T., Zarzeka-Raczkowska E., *Hybrid adhesive bonded and riveted joints – influence of rive geometrical layout on strength of joints,* Archives of Metallurgy and Materials, 2012, 1127-1135.
18. Sadowski T., Balawender T., Śliwa R., Golewski P., Kneć M., *Modern hybrid joints in aerospace: modelling and testing*, Archives of Metallurgy and Materials, 2013, 163-169.

TIAM kwartalnik naukowo-techniczny
TECHNOLOGIA I AUTOMATYZACJA MONTAŻU
ZESPOŁÓW • MASZYN • URZĄDZEŃ

Izabela Miturska-Barańska[1], Anna Rudawska[2],
Elżbieta Doluk[3], Jacek Ogrodniczek[4]

DOI: 10.7862/tiam.2022.3.2

IMPACT OF ADHESIVE TYPE AND ABRASIVE WEAR USED IN THE SURFACE PREPARATION PROCESS ON THE STRENGTH OF STEEL SHEET ADHESIVE JOINTS

WPŁYW RODZAJU KLEJU I ZUŻYCIA ŚCIERNIWA STOSOWANEGO W PROCESIE PRZYGOTOWANIA POWIERZCHNI NA WYTRZYMAŁOŚĆ POŁĄCZEŃ KLEJOWYCH BLACH STALOWYCH

Abstract

The aim of the paper was to present issues related to the determination of the influence of selected technological factors: the method of surface preparation and type of adhesive on the strength of adhesive joints made of steel sheet C45. As a method of surface preparation the process of shot-blasting with the use of three types of abrasives differentiated in terms of the degree of its wear was used. The adhesive bonds were made with the use of two two-component epoxy adhesive compositions based on Epidian 57 epoxy resin and PAC and Z-1 curing agents combined with the resin in the recommended proportions. The measurements of roughness and topography of surfaces prepared for the bonding process were also carried out. After the curing process, strength tests of adhesive bonds were performed on the Zwick/Roell 150 testing machine, according to PN-EN 1465 standard. It was noted, among others, that with increasing wear of the abrasive used in the surface preparation process, the value of adhesive bonds strength decreased and the higher strength of adhesive bonds was characterized by adhesive joints made with Epidian57/Z-1/100:10 adhesive. The obtained results were subjected to statistical analysis.

Keywords: adhesive joints, C45 steel sheet, tensile strength, shot blasting

Streszczenie

Celem artykułu było przedstawienie zagadnień związanych z określeniem wpływu wybranych czynników technologicznych: sposobu przygotowania powierzchni oraz rodzaju kleju na wytrzymałości połączeń klejowych wykonanych z blachy stalowej C45. Jako sposób przygotowania powierzchni wykorzystano proces śrutowania z wykorzystaniem trzech rodzajów ścierniw zróżnicowanych pod względem stopnia jego zużycia. Połączenia klejowe wykonano przy użyciu dwóch dwuskładnikowych kompozycji klejowych epoksydowych bazujących na żywicy epoksydowej Epidian 57 oraz utwardzaczy PAC i Z-1 łączonych z żywicą w zalecanych proporcjach. Przeprowadzono także pomiary chropowatości oraz topografii powierzchni przygotowanych do procesu klejenia. Po procesie utwardzania dokonano prób wytrzymałościowych połączeń klejowych na maszynie wytrzymałościowej Zwick/Roell 150, zgodnie z normą PN-EN 1465. Zauważono m.in., że wraz ze wzrostem stopnia zużycia ścierniwa użytego w procesie przygotowania powierzchni, wartość wytrzymałości połączeń klejowych malała, a wyższą wytrzymałością charakteryzowały się połączenia klejowe wykonane przy użyciu kleju Epidian57/Z-1/100:10. Uzyskane wyniki poddano analizie statystycznej.

Keywords: połączenia klejowe, blacha stalowa, wytrzymałość, śrutowanie

[1] Izabela Miturska-Barańska, Lublin University of Technology, Faculty of Mechanical Engineering, Nadbystrzycka 36, 20-618 Lublin, PL, ORCID: 0000-0003-4140-4768, *i.miturska@pollub.pl
[2] Anna Rudawska, Lublin University of Technology, Faculty of Mechanical Engineering, Nadbystrzycka 36, 20-618 Lublin, PL, ORCID: 0000-0003-3592-8047.
[3] Elżbieta Doluk, Lublin University of Technology, Faculty of Mechanical Engineering, Nadbystrzycka 36, 20-618 Lublin, PL, ORCID: 0000-0003-2605-1394.
[4] Jacek Ogrodniczek, Lublin University of Technology, Faculty of Mechanical Engineering, Nadbystrzycka 36, 20-618 Lublin, PL, ORCID: 0000-0002-6484-2245.

1. Introduction

There are many methods of joining structural components. For this purpose, assembly methods such as welding, riveting, welding, soldering or adhesive bonding can be used. It is important to choose the right method to ensure that the joints have the expected properties. However, the selected method must not adversely affect the specific properties of the structure, which include, but are not limited to: the dimension of the construction, shape, functionality, usability, reliability, aesthetics, modularity and universality [1–4].

One of the oldest and most frequently used methods of joining construction materials is adhesive bonding. Adhesives, as adhesive plastics, have the ability to create adhesive forces on the components to be bonded. The process of adhesive bonding consists in applying a thin layer of adhesive substance between the surfaces to be bonded, which connects them by means of adhesive forces and cohesion force, i.e. the force of internal coherence of the materials [5]. In addition, adhesives used in joints provide corrosion protection and can be used as sealants. A number of factors influence the effectiveness of the bonding process and the properties of the joints. Technological, construction, material and operational factors are among them. These factors include: the method of surface preparation of the materials to be bonded, the type of adhesive together with the method of its application on the surfaces to be bonded, as well as the curing conditions of the adhesive joint depending on the type of adhesive (temperature, time and pressure) and the conditions of seasoning [6, 7]. Changes to these factors during the bonding process may affect the properties of certain joints in different ways. However, due to the specification of the joints under consideration, it is necessary to conduct studies to analyse the effects of these factors on specific cases and applications. A change in these factors for a particular joint may affect the properties of the joint, e.g. another material, in a slightly different way, including its strength properties [8, 9].

Analyzing the technological process of adhesive bonding, special attention should be paid to the preparation of the surface. The process of surface preparation consists in removing the surface layer of oxides and other impurities occurring in the form of lubricants, dusts, sediments, oils, microorganisms, moisture, etc [3]. The main distinguishing features are mechanical and chemical cleaning, as well as special treatments dedicated to specific materials. Mechanical cleaning is, for example, machining with an abrasive bulk tool, sandblasting, shotblasting, flame burning or machining [10–12]. Chemical cleaning is carried out using solvents such as: petrol, acetone, benzene, various types of detergents, trichloroethylene [13–15]. The surface preparation process significantly affects the adhesive properties of the bonded materials and the strength of the adhesive joints. Thanks to appropriate surface preparation, it is possible to obtain properly made adhesive joints and to ensure adequate joint strength, of course, while also complying with other structural and technological conditions [8]. Appropriate surface preparation increases the durability of the joint and determines the reliability of the joint.

In this paper the analysis of the influence of abrasive wear used in the surface preparation process and the effects of the adhesive type on selected strength aspects of C45 steel sheets adhesive joints is considered.

2. Studies methods

2.1. Characteristics of adhesive joints and bonded material

In the experimental studies, single-overlapping adhesive joints were made. The joints were made of low carbon steel sheets C45 (1.0503). C45 steel is one of the higher quality structural steels. Unalloyed quality steel is used for heat-treatment, easy to process but hardly weldable. It is mainly used in machine elements and equipment of medium load e.g. tools, knives, shafts, screws, discs, levers, gears, crankshafts, spindles, woodworking tools [12, 16–18]. The chemical composition and some physical properties of the used material (according to PN EN 10020:2003) are presented in Table 1.

Table 1. Chemical composition and physical properties of C45 steel [19]

Stainless steel C45			
Chemical composition, %		**Physical properties**	
C	0.44	Rm	638 MPa
Mn	0.55		
Si	0.21		
P	0.01	Re	369 MPa
S	0.02		
Cr	0.16		
Ni	0.24	Hardness	255 HB
Cu	0.07		

The subject of the study were single overlap adhesive joints loaded on shear as shown in Figure 1.

The length of the overlap was assumed to be 15 mm, and the thickness of the adhesive layer to be about 0.2 mm. The area of adhesive and the thickness of the adhesive joint were verified before the strength tests.

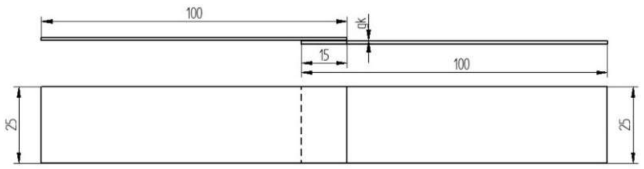

Fig. 1. Single overlap adhesive bond of steel sheet C45

2.2. Method of steel sheet surface preparation

Surface preparation is one of the first stages in the process of making permanent adhesive bonds. Several processes connected with cleaning and geometric development of joined elements' surfaces in the presented studies. The surface development of the used samples was achieved by mechanical shotblasting process, where the used abrasive was corundum of various degrees of wear. An abrasive is a fine grain of an abrasive material, which is the basis for the construction of abrasive tools. Electrocorundum (Al_2O_3) is one of the most common and cheapest abrasives. It is a synthetic version of a mineral called corundum. Corundum in its pure form is used only for polishing, sometimes for tool sharpening [20, 21]. Corundum grains have sharp edges and controlled properties. It consists mainly of aluminium oxide. The shotblasting process was carried out with an AUER shotblasting machine. The blasting pressure was 0.6 MPa and the nozzle distance was 100 mm. During the shotblasting process, the samples were divided into 3 groups because 3 types of abrasive were used, differentiated in the level of wear. The abrasive wear was estimated as small, medium and high, depending on the time it was working. The classification into particular variants of shotblasting is presented in Table 2.

Table 2. Shotblasting variants according to wear of the abrasive used to prepare steel sheet surface

Shotblasting	Level of wear	Operating time of abrasive
Variant 1	Small	24 hours (1 days)
Variant 2	Medium	496 hours (3 months)
Variant 3	High	992 hours (6 months)

The next step in the surface preparation process, after machining, was degreasing the surface. Degreasing is one of the most frequently used surface preparation operations performed just before the joining process, because it removes all kinds of dust and grease impurities, often remaining after previous processing [14, 19]. Degreasing of steel sheet surfaces intended for bonding was carried out with technical acetone by spraying three times. For the first two replications the degreasing agent was removed with a dust-free fabric, while after the third spraying the samples were allowed to self-evaporate and completely dry.

2.3. Characteristics of the used adhesive

Two types of epoxy adhesive compositions were used to make adhesive joints, which were the subject of the study. The base for both adhesives was Epidian 57 epoxy resin. This resin occurs in the form of viscous liquid of light yellow colour and characteristic smell of styrene. Its basic features are: very good mechanical strength, high resistance to chemical substances such as oils, greases, acids, etc., proper adhesion to the substrate and good hardness of the obtained adhesive coating, very good adhesive joints of various materials such as ceramics, metal, glass, wood, possibility of hardening at ambient temperature. The epoxy number of Epidian 57 is 0.40 mol/100g, density at 20°C is in the range of 1.14-1.17 g/cm3, and viscosity at 25°C - 13 000 - 19 000 mPas [22, 23].

The resin must be properly mixed with the cure agent in order to cross-link and harden. The first adhesive composition used for the adhesive bonds consisted of the resin and PAC hardener. PAC hardener is a viscous liquid with an amber colour and characteristic amine smell. When used with epoxy resins, the PAC hardener is used for joining elements exposed to deformation, e.g. bonding thin sheets, joining rubber with metal, in compositions for flooding elements in electrical and electronic engineering [19, 24]. The preparation of the composition was based on mixing Epidian 57 epoxy resin and PAC hardener at a weight ratio of 100:80. In the further part of the paper the composition determination – Epidian57/PAC/100:80 was used. The second composition was prepared with the use of Z-1 hardener. This is a viscous liquid of light yellow colour and characteristic smell for triethylenetetraamine. The Z-1 hardener is used primarily in connection with low-molecular weight epoxy resins and for joints exposed to deformation, such as joining thin sheets, joining rubber with metal or plywood [19, 24]. It is also used to harden liquid epoxy resins. The composition was prepared at a proportion by weight to resin ratio of 100:10 - Epidian57/Z-1/100:10.

Epidian57/PAC/100:80 adhesive composition is much more slow-bonded than Epidian57/Z-1/100:10 composition. PAC curing agent is one of the slow-reacting hardeners. After about 12 hours the initial hardening of the composition takes place and after 72 hours it reaches the hardening of 80 - 90%. The total cure lasts from 7 to 14 days. This process can be accelerated by increasing the temperature after the first curing step. In case of gelation of compositions containing Z-1 hardener this time is about 35 minutes at ambient temperature. Initial cure (degree of cure 80-90%) is achieved after 48 hours. However, the total cure lasts 7-14 days. It should also be noted that adhesive compositions containing PAC hardener are characterized by higher elasticity, higher impact resistance and lower resistance to elevated temperature than compositions hardened with Z-1 curing agent.

The preparation of two-component adhesive compositions was based on a precise mixing of epoxy resin with a selected hardener at an appropriate weight ratio. The OP-2 laboratory scale with the accuracy of 0.01 g was used to weigh the necessary amount of adhesive compositions components. Both compositions were mixed with a mechanical turbine mixer with two blades during 3 minutes at a speed of 460 rpm. The adhesive compositions were prepared just before the process of adhesive bonding. They were applied manually to one of the joined surfaces with a serrated polymer float, keeping constant thickness over the whole joined surface.

2.4. Conditions for performing and testing adhesive bonds

The bonding process was carried out in laboratory conditions at 26 ± 1°C with a humidity of 32%. The samples were conditioned to harden the joint for 7 days under 0.14 MPa pressure. After this time, the samples were subjected to strength tests. A tensile shear test was performed on a Zwick/Roell Z150 testing machine. The test was carried out in accordance with DIN EN 1465 standard at a crosshead speed of 5 mm/min. For each variant of surface preparation and for each type of adhesive, 10 single overlap adhesive bonds were made. Additionally, prior to the bonding process, the surface roughness and topography were measured using the T8000 RC 120-140 from Hommel-Etamic. Measurements were taken for 3 randomly selected samples from each variant of surface preparation.

3. Results of research

3.1. Roughness measurements results

The measurements of roughness and surface topography were performed in accordance with PN-EN ISO 13565-2:1999. The length of the measurement distance was ln = 4.8 mm and the elementary distance lr = 0.8 mm. The analyzed surface roughness parameters were: Ra - arithmetic mean of the ordinates of the roughness profile, Rt - total height of the roughness profile and Rp - height of the highest elevation of the profile [25, 26].

Figure 2 shows the influence of the abrasive wear level used in the surface preparation process on the Ra roughness parameter. Considering the results obtained, it can be observed that the value of the arithmetic mean of the ordinate decreases with increasing wear of the abrasive used for surface preparation of the samples. The use of an abrasive that has operated for 6 months (variant 3) resulted in a 44% decrease in the Ra parameter in relation to the Ra parameter value for variant 1, where the abrasive wear rate was small.

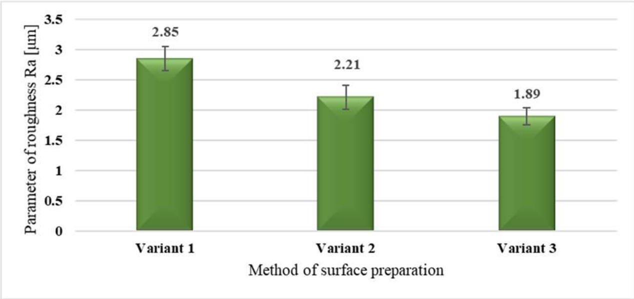

Fig. 2. Effect of abrasive wear level of the abrasive used in the surface preparation process on the arithmetic average of the ordinates roughness profiles (Ra)

Considering the height parameters of the surface roughness profile Rt, Rp, it should be noted that similarly to the Ra parameter, the value of the parameters decreases with increasing abrasive wear, as shown in Figure 3.

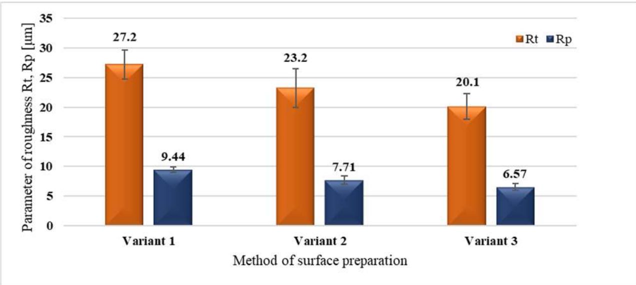

Fig. 3. Effect of the abrasive wear level of the abrasive used in the surface preparation process on the height parameters of the roughness profile (Rt, Rp)

Shotblasting affects the lack of direction of the surface geometric structure (Fig. 4). The shotblasting operation has resulted in many peaks and cavities with sharp peaks and valleys on the surface, which can be better detected in the surface profilograms (Fig. 5).

Taking into account the presented results of roughness measurements and surface topography, it can be expected that such a shaped surface may be a surface with good adhesion properties. This can be proved by the undirected geometric structure of the surface characterized by numerous peaks and valleys, which positively influences the penetration and anchoring of the adhesive [19, 27, 28].

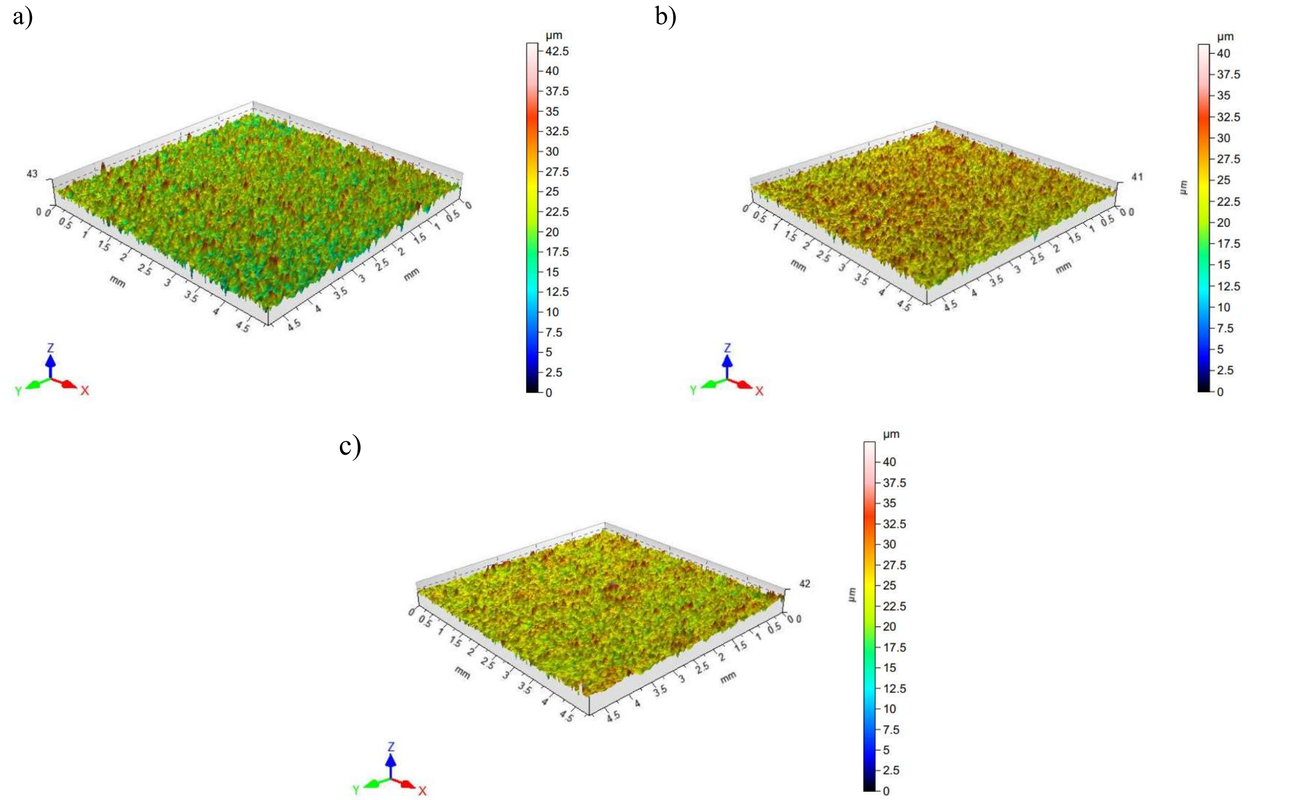

Fig. 4. Influence of the abrasive wear level of the surface preparation process on the surface topography (a) variant 1 - small abrasive wear level, (b) variant 2 - medium abrasive wear level, (c) variant 3 - high abrasive wear level

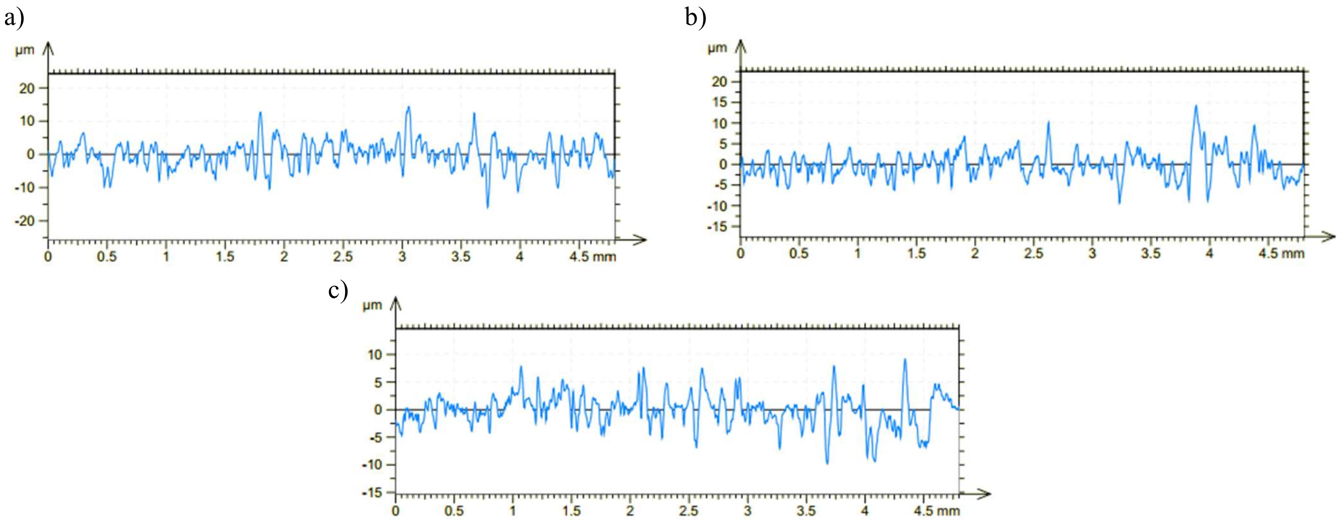

Fig. 5. Surface profilograms after blasting a) variant 1 - small abrasive wear, b) variant 2 - medium abrasive wear, c) variant 3 - high abrasive wear

3.2. Strength test results

After a period of time, when the adhesive joint achieved complete curing, the adhesive joints were subjected to destructive strength tests. The results are shown in Figure 6.

On the basis of the strength results obtained, it can be observed that with the increase in abrasive wear level, the strength of adhesive bonds decreased. For both adhesives, the highest strength was obtained in the case of samples whose surfaces were subjected to 1 shotblasting variant, i.e. with the lowest abrasive wear. The adhesive bonds made with Epidian57/ Z-1/100:10 adhesive were characterized by higher strength. This may result from different properties in comparison with the second adhesive used - Epidian57/PAC/100:80, which is characterized by

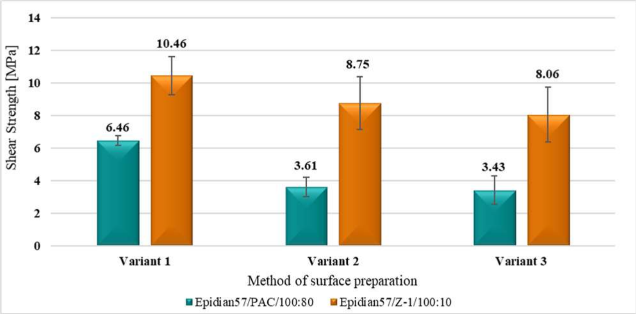

Fig. 6. Results of shear strength of steel sheet adhesive joints made with two epoxy adhesives due to the abrasive wear level of the abrasive used in the surface preparation process

higher elasticity but also higher viscosity. For this reason, the penetration of the adhesive into the surface cavities along the length of the adhesive overlap may have been more problematic. It should be noted, however, that despite the differences between the strength of joints made with both adhesives, the distribution of these values is similar in both cases - the value of strength decreases with increasing abrasive wear. An important aspect worth emphasizing is also the repeatability of the results. In the case of samples prepared for the bonding process with variant 1, the repeatability of the results is much higher than in the case of the other two variants. The value of standard deviation for Epidian57/PAC/100:80 adhesive is 0.30 MPa for variant 1 (which constitutes 4.71% of average strength), 0.61 MPa for variant 2 (which constitutes 17.02% of average strength), 0.87 MPa for variant 3 (which constitutes 25.5% of average strength). For Epidian57/Z-1/100:10 the values of standard deviations were as follows: for variant 1 - 1.16 MPa (which constitutes 11.18% of mean strength), for variant 2 - 1.62 MPa (which constitutes 18.53% of mean strength), for variant 3 - 1.67 MPa (which constitutes 20.80% of mean strength). It can be noticed that higher repeatability of the results was obtained in the case of joints made with Epidian57/PAC/100:80 adhesive.

3.3. Statistical analysis of the obtained results

The strength of adhesive bonds is an important factor in the evaluation of such bonds. However, in order to be able to compare the results obtained, it is necessary to analyze them statistically.

At the beginning, the distribution normality of the obtained results was checked with the assumed confidence level of $\alpha = 0.05$. For this purpose, the Shapiro-Wilk test was used. Results of this test are presented in Table 3.

The analysis of the conformity of empirical distribution with the normal distribution by Shapiro--Wilka test did not reject the hypothesis of the normality of strength distributions of the tested adhesive bonds for the analysed methods of surface preparation ($p>\alpha$). The next step was to check the variances homogeneity using the Levene test, which also did not reject the hypothesis about the equality of variances. Therefore, ANOVA statistics were carried out in order to verify the occurrence of significant differences in the influence of abrasive wear on the strength of adhesive joints in the process to prepare the surfaces of the joined elements and the type of adhesive. Post-hoc Tukey test was carried out to determine homogeneous groups of distribution. The results of this test are presented in Table 4.

Table 3. Normality test - adhesive joints' strength

Shotblasting	Type of adhesive	Shapiro--Wilk statistics W	Probability level p	Normality of distribution
Variant 1	Epidian57/ PAC/100:80	0.836298	0.184825	Yes
	Epidian57/ Z-1/100:10	0.908799	0.476064	Yes
Variant 2	Epidian57/ PAC/100:80	0.786330	0.079880	Yes
	Epidian57/ Z-1/100:10	0.788513	0.083166	Yes
Variant 3	Epidian57/ PAC/100:80	0.841345	0.199353	Yes
	Epidian57/ Z-1/100:10	0.843504	0.205812	Yes

Table 4. The post-hoc Tukey's test designating homogenous groups

Shotblasting	Type of adhesive	Average shear strength [MPa]	Homogenous groups	
			a	b
Variant 1	Epidian57/ PAC/100:80	6.46	****	
	Epidian57/ Z-1/100:10	10.46		****
Variant 2	Epidian57/ PAC/100:80	3.61	****	
	Epidian57/ Z-1/100:10	8.75		****
Variant 3	Epidian57/ PAC/100:80	3.43	****	
	Epidian57/ Z-1/100:10	8.06		****

On the basis of the obtained results it can be noticed that the strength results for the samples bonded with Epidian57/PAC/100:80 adhesive for all shotblasting variants are in one group and for Epidian57/ Z-1/100:10 adhesive in the other group. This means that at a given confidence level $\alpha = 0.05$ the abrasive wear level does not significantly affect the change of strength properties of the obtained joints. In this case, the type of adhesive has a bigger influence.

4. Conclusions

The conducted research concerned the influence of abrasive wear in the abrasive processing process on the static strength of overlapping adhesive joints of C45 steel sheets. Variable factors in the study were: the method of surface preparation for adhesive bonding and the type of adhesive. As a method of surface preparation, the shotblasting process was used with the use of three types of abrasives differentiated in their wear level. Two types of two-component epoxy adhesive compositions based on Epidian 57 epoxy resin with PAC and Z-1 curing agents added to the resin in appropriate proportions, according to the manufacturer's recommendations, were used as a binder. Measurements of roughness and topography of surfaces prepared for the bonding process were also carried out. Based on the tests carried out, it can be seen that:

- the roughness parameters decrease with increasing wear of the abrasive used in the surface preparation of the samples to be bonded,
- shotblasting is a process that positively influences the development of the surface to be bonded, which can be a surface with good adhesive properties,
- with the increase in the level of abrasive wear used in the process of surface preparation, the value of strength of adhesive bonds decreased,
- higher strength was characterized by adhesive bonds made with the use of a less lightweight adhesive, i.e. Epidian57/Z-1/100:10. However, higher repeatability of results was obtained in the case of bonds made with Epidian57/PAC/100:80 adhesive.

To summarize, it should be stated that mechanical processing has a significant impact on the strength of adhesive joints made of structural sheet. This is due to the formation of more micro roughness, which contributes to a better anchoring of the adhesive in such a surface, bearing in mind that this is also related to the type of adhesive used. The degree of abrasive wear and tear in the process of shotblasting the connected elements resulted in a deterioration of the obtained adhesive strength results of steel sheet joints. However, the statistical analysis showed that at the set confidence level $\alpha = 0.05$ these differences are not considered significant. In this case, the type of adhesive has more influence.

References

1. Rudawska A., Miturska I., Semotiuk L., The influence of adhesive type and surface treatment on the strength of c45 steel sheets adhesive joints. Technologia i Automatyzacja Montażu. 2019;(2):34–7.
2. Patil O.R., Ameli A., Datla N.V., Predicting environmental degradation of adhesive joints using a cohesive zone finite element model based on accelerated fracture tests. International Journal of Adhesion and Adhesives. 2017; 76:54–60.
3. Ebnesajjad S., redaktor. Handbook of adhesives and surface preparation: technology, applications and manufacturing. Amsterdam: William Andrew/Elsevier; 2011. 427 s. (PDL handbook series).
4. Hashim S.A., Adhesive bonding of thick steel adherends for marine structures. Marine Structures. 1999;12(6): 405–23.
5. Silva L.F.M. da, Öchsner A., Adams R.D., redaktorzy. Handbook of adhesion technology. Heidelberg: Springer; 2011.
6. Landrock A.H., Ebnesajjad S., Adhesives technology handbook. Third edition. Amsterdam ; Boston: Elsevier/ WA, William Andrew is an imprint of Elsevier; 2015.
7. Kuczmaszewski J., Fundamentals of metal-metal adhesive joint design. Lublin: Lublin University of Technology : Polish Academy of Sciences, Lublin Branch; 2006.
8. da Silva Lucas F.M., Carbas R.J.C., Critchlow G.W., Figueiredo MAV, Brown K. Effect of material, geometry, surface treatment and environment on the shear strength of single lap joints. International Journal of Adhesion and Adhesives. wrzesień 2009;29(6):621–32.
9. Rudawska A., Maziarz M., Miturska I., Impact of Selected Structural, Material and Exploitation Factors on Adhesive Joints Strength. Kulisz M., Szala M., Badurowicz M., Cel W., Chmielewska M., Czyż Z., i in., redaktorzy. MATEC Web Conf. 2019;252:01006.
10. Brack N., Rider A.N., The influence of mechanical and chemical treatments on the environmental resistance of epoxy adhesive bonds to titanium. International Journal of Adhesion and Adhesives. styczeń 2014;48:20–7.
11. Rudawska A., Reszka M., Warda T., Miturska I., Szabelski J., Stančeková D., i in. Milling as a method of surface pretreatment of steel for adhesive bonding. Journal of Adhesion Science and Technology. grudzień 2016;30(23): 2619–36.
12. Rotella G., Alfano M., Schiefer T., Jansen I., Evaluation of mechanical and laser surface pre-treatments on the strength of adhesive bonded steel joints for the automotive industry. Journal of Adhesion Science and Technology. 2 kwiecień 2016;30(7):747–58.
13. Litchfield R.E., Critchlow G.W., Wilson S., Surface cleaning technologies for the removal of crosslinked epoxide resin. International Journal of Adhesion and Adhesives. sierpień 2006;26(5):295–303.
14. Rudawska A., Miturska I., The influence of degreasing and machining treatment on the adhesive joint strength. Przetwórstwo Tworzyw. 2018;24(2):38–46.
15. Brack N., Rider A.N., The influence of mechanical and chemical treatments on the environmental resistance of epoxy adhesive bonds to titanium. International Journal of Adhesion and Adhesives. styczeń 2014;48:20–7.

16. Kozma L., Olefjord I., Surface treatment of steel for structural adhesive bonding. Materials Science and Technology. listopad 1987;3(11):954–62.
17. Habig K.-H., Chemical vapor deposition and physical vapor deposition coatings: Properties, tribological behavior, and applications. Journal of Vacuum Science & Technology A: Vacuum, Surfaces, and Films. 2006;4(6): 2832–43.
18. Leppert T., Effect of cooling and lubrication conditions on surface topography and turning process of C45 steel. International Journal of Machine Tools and Manufacture. 2011;51(2):120–6.
19. Rudawska A., Miturska I., Impact study of single stage and multi stage abrasive machining on static strength of lap adhesive joints of mild steel. Stančeková D., Vaško M., Rudawska A., Čuboňová N., Sapietová A., Mrázik J., i in., redaktorzy. MATEC Web Conf. 2018;244:02006.
20. Lu P.J., Yao N., So J.F., Harlow G.E., Lu J.F., Wang G.F., i in. The Earliest Use of Corundum and Diamond. Archaeometry. 2005;47(1):1–12.
21. Shannon R.D., New high pressure phases having the corundum structure. Solid State Communications. 2006; 4(12):629–30.
22. de Bruyne N.A., The adhesive properties of epoxy resins. J Appl Chem. 2007;6(7):303–10.
23. Ellis B., redaktor. Chemistry and Technology of Epoxy Resins. Dordrecht: Springer Netherlands; 1993.
24. Miturska I., Rudawska A., Mechanical properties of selected epoxy adhesives. Informatyka, Automatyka, Pomiary w Gospodarce i Ochronie Środowiska. 2017;7(4): 88–91.
25. Sedlaček M., Podgornik B., Vižintin J., Influence of surface preparation on roughness parameters, friction and wear. Wear. 2009;266(3–4):482–7.
26. Gadelmawla E.S., Koura M.M., Maksoud T.M.A., Elewa I.M., Soliman H.H., Roughness parameters. Journal of Materials Processing Technology. 2002;123(1):133–45.
27. Shahid M., Hashim S.A., Effect of surface roughness on the strength of cleavage joints. International Journal of Adhesion and Adhesives. 2002;22(3):235–44.
28. Sancaktar E., Gomatam R., A study on the effects of surface roughness on the strength of single lap joints. Journal of Adhesion Science and Technology. 2001;15(1): 97–117.

TiAM kwartalnik naukowo-techniczny
TECHNOLOGIA I AUTOMATYZACJA MONTAŻU
ZESPOŁÓW • MASZYN • URZĄDZEŃ

Adam Barylski[1]

DOI: 10.7862/tiam.2022.3.3

PROBLEMS ASSOCIATED WITH THE HEATING UP OF ACTUATING SYSTEM OF A SINGLE-DISC LAPPING MACHINE FOR FLAT SURFACES

PROBLEMATYKA NAGRZEWANIA SIĘ ELEMENTÓW UKŁADU WYKONAWCZEGO DOCIERARKI JEDNOTARCZOWEJ DO PŁASZCZYZN

Abstract

The paper presents the results of the examination of the heating up of the basic elements of the actuating system of a single-disc lapping machine with standard kinematics, intended for machining flat surfaces. The increase of the temperature of the drive assembly, rollers and separator guide ring, as well as the lapping disc and machined elements were analysed. Heating up of the machining system was examined during the machining of a cast iron tool and flat surface lapping. Lapping is one of the methods of abrasive machining applied during the individual fitting of elements in assembly or when a technological compensator is used. The increase of temperature in the machining system influences, among others, the dimensional accuracy of lapped metal elements.

Keywords: mechanical engineering, assembly technologies, lapping, temperature, analysis

Streszczenie

Przedstawiono wyniki badań nagrzewania się podstawowych elementów układu wykonawczego docierarki jednotarczowej o standardowej kinematyce do obróbki powierzchni płaskich. Analizowano przyrost temperatury zespołu napędowego, rolek i pierścieni prowadzących separatory oraz tarczy docierającej i obrabianych elementów. Badano nagrzewanie się układu obróbkowego podczas wyrównywania żeliwnego narzędzia i docierania powierzchni płaskich. Docieranie jest jedną z metod obróbki ściernej stosowaną podczas indywidualnego dopasowywania elementów w montażu lub przy wykorzystaniu kompensatora technologicznego. Przyrost temperatury w układzie obróbkowym ma między innymi wpływ na dokładność wymiarową docieranych elementów metalowych.

Słowa kluczowe: inżynieria mechaniczna, technologie montażowe, docieranie, temperatura, analiza

1. Introduction

One of machining methods applied during the assembly of components is lapping with a loose abrasive [1]. This technology has been applied during individual fitting of elements of a construction or during assembly of a technological compensator. In the case of a unilateral machining of flat surfaces, it is conducted on a single-disc lapping machines where standard actuating system consists of a ring system [2]. Guiding rings, from one to four, with machined elements placed in separators are set in motion directly through the revolving lapping disc. The rings are also applied to dress the surface of an active lapping disc [2].

Current production and examinations include lapping machines featuring water cooling of the metal lapping disc [3, 4], as well as machines without forced cooling. The second solution eliminates problems with possible corrosion of the lapping machine elements. The main source of heat during lapping of flat surfaces, apart from the very process of grinding by abrasive grains (interaction of the abrasive with machined material and the material of the lapping disc) is the worm gear – acting as a drive system of the machine.

Changing temperature of the elements of a lapping system significantly influences the yielded dimensional accuracy of lapped elements. Knowledge of the temperature increase pattern (and consequently the

[1] Professor Adam Barylski, PhD, DSc, ME – Gdansk University of Technology, Faculty of Mechanical Engineering and Ship Technology, G. Narutowicza 11/12, 80-233 Gdańsk, abarylsk@pg.edu.pl, ORCID: 0000-0003-1672-8445.

expansion of the lapped metal elements) can facilitate the selection of place and time of the control of linear dimensions, as well as determination of the machining dimension in the technological documentation of assembly.

2. Test stand

The examinations of the heating up of lapping machine elements [5] were conducted using a single-disc lapping machine Abralap 380 and thermal vision camera Optris PI200 (fig. 1).

An increase of the temperature of the actuating system and driving assembly of the lapping machine was analysed (fig. 2). During the examination, abrasive paste based on aluminium oxide (500 Grit Aluminium Oxide) produced by States Products Co was applied.

Fig. 1. General view of the test stand: 1 - single-disc lapping machine, 2 - thermal vision camera, 3 - camera stand, 4 - guiding ring rotational speed sensor, 5, 6 - device recording the rotational speed of the lapping disc and guiding rings, 7 - laptop computer

a) b) c)

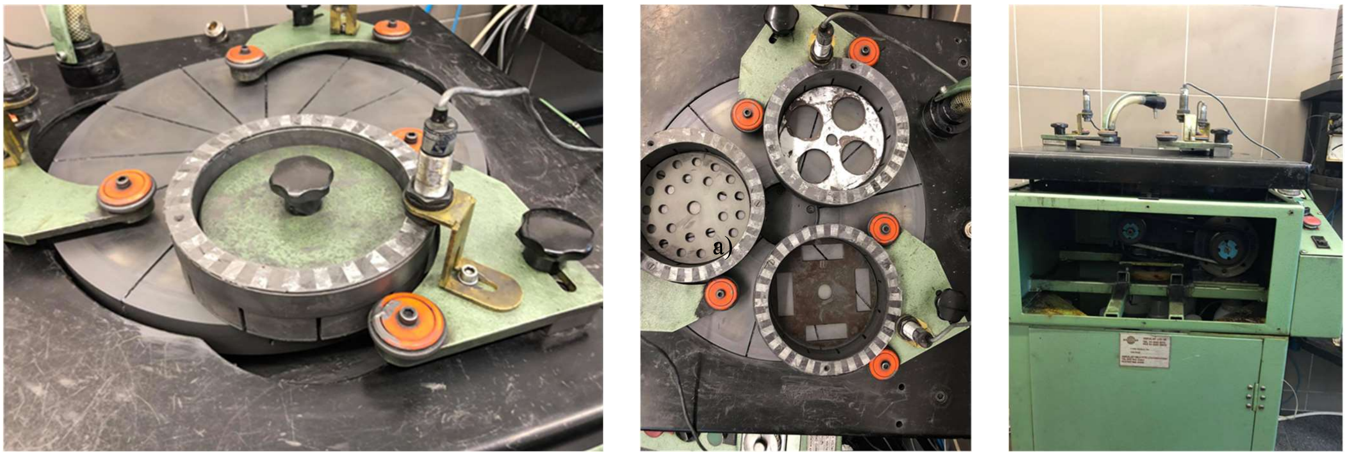
Fig. 2. View of: a) guiding ring containing machined elements and their ballast loads b) separators placed in the three guiding rings, c) uncovered drive system of Abralap 380 lapping machine

3. Results of the examinations

3.1. Heating of the drive assembly of the lapping machine in idle mode

Figures 3-6 show the results of the measurements of average temperature of the elements of the lapping machine drive assembly, both before initiating the examinations and, e.g. after 20 minutes of operation in the idle mode and for two values of the rotational speed of the lapping disc n_t. The distance between the thermal vision camera and the analysed drive assembly was 1 m.

In analysed situation presented in fig. 3b, V-belt heated up to, on average, 48ºC, driving pulley to 48.6ºC, and driven pulley to 49ºC. The average temperature of the electric motor was 39.8ºC and of the worm gear (driving the lapping disc) - 45ºC. After increasing the rotational speed of the lapping disc to $n_t = 80\ min^{-1}$ the temperature if the belt drive increased by 1.95ºC/min (fig. 4). In the examined system, the temperature of the V-belt after 20 minutes of operation was 64ºC, the temperature of the driving pulley was 64.4ºC, the temperature of the driven pulley reached 65ºC, electric motor temperature was 52ºC, and the temperature of the worm drive was 59ºC.

a) b)

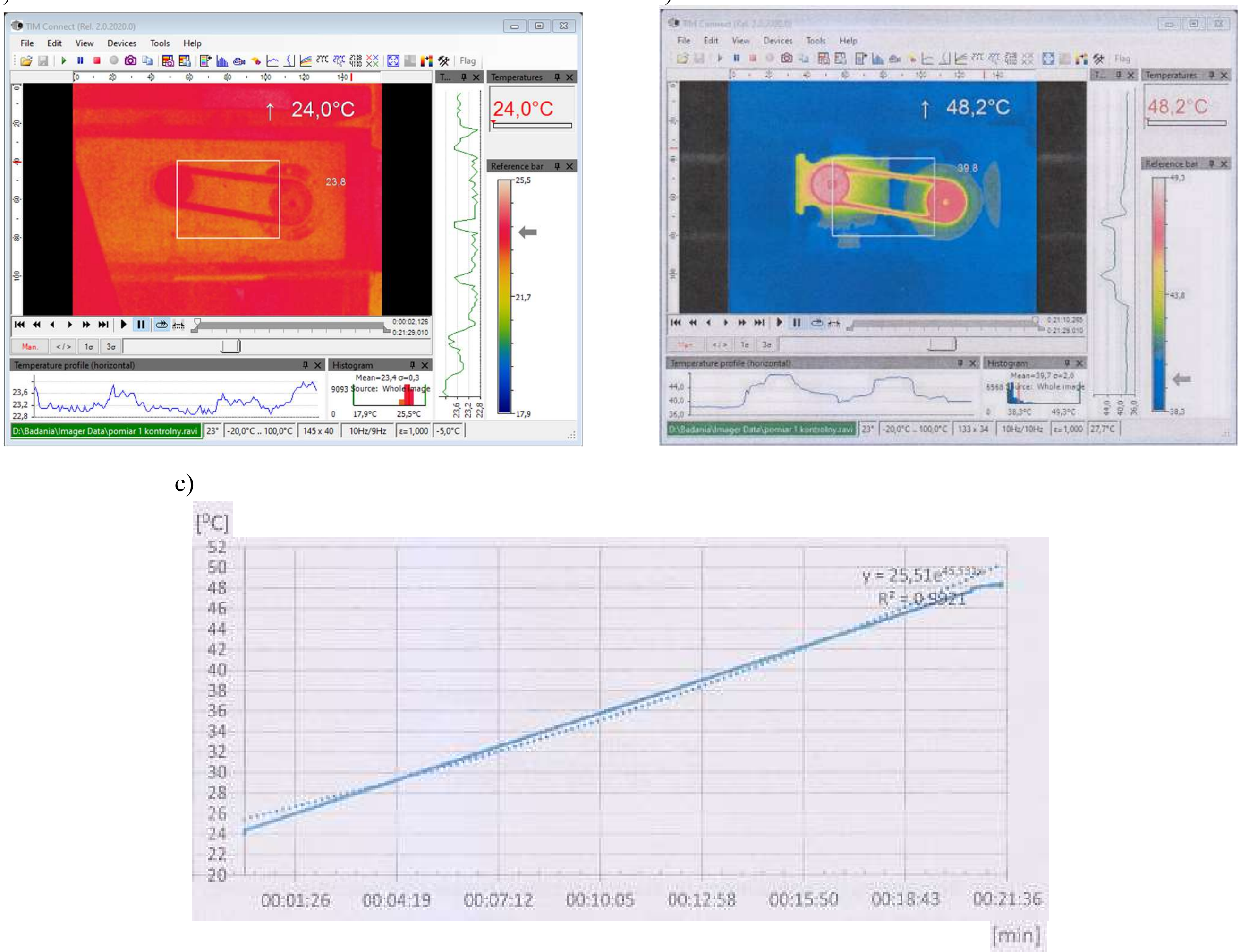

Fig. 3. Results of the measurements of the temperature of the lapping machine drive assembly: a) initial moment, b) after 20 minutes of operation without placing the guiding rings on the lapping disc (n_t = 40 min^{-1}), c) the graphic representation of the increase of the temperature of the belt drive in time (on average, 1.2ºC/min)

a) b)

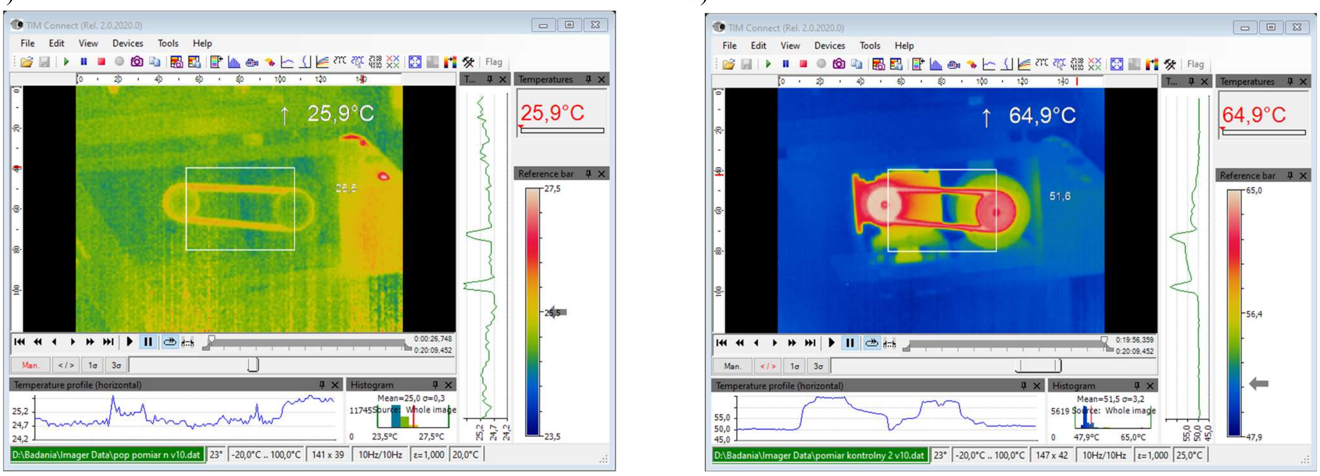

Fig. 4. Results of the measurements of the temperature of the drive system of the lapping machine: a) in the initial moment, b) after 20 minutes, without guiding rings placed on the lapping disc (n_t = 80 min^{-1})

3.2. Heating up of the drive system and lapping disc during dressing

During dressing of the lapping disc (with guiding rings) a dosage of abrasive was refilled manually (using an appropriate brush). Due to a 7-minute break in the operation of the lapping disc (between 12th and 18th minute of dressing) further increase of the temperature of the drive system elements was less intensive (fig. 5). The maximum temperature of the driven pulley was 44ºC, of the V-belt 43ºC, of the driving pulley 42.5ºC, of the electric motor and of worm gear 36ºC. When rotational speed of the lapping disc increased to 80 min^{-1}, the increase of the V-belt temperature was 1.65ºC/min (fig. 6), while the average temperature of the driving pulley increased to 58ºC, the temperature of the electric motor increased to 49ºC and the temperature of the worm gear reached 51ºC (the break in operation of the lapping disc for refilling the abrasive was 5.5 minutes).

a)

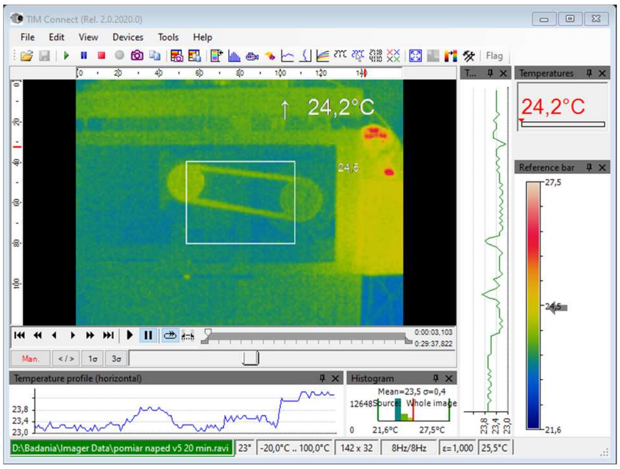

b)

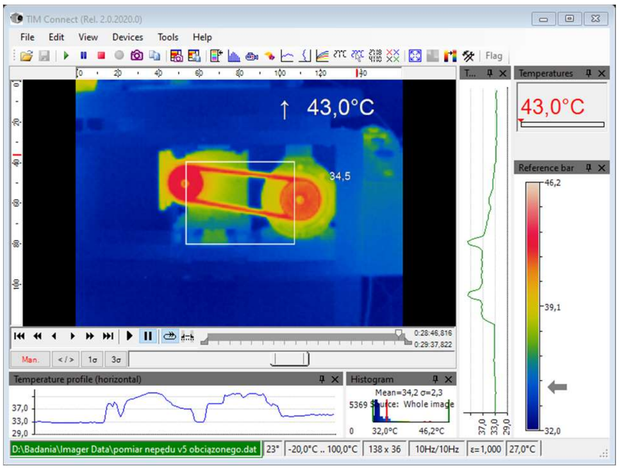

c)

Fig. 5. Results of the measurements of the temperature of the lapping machine drive system: a) in the initial moment, b) after 20 min of dressing the lapping disc with guiding rings (n_t = 40 min^{-1}) and manual refilling of the abrasive after 12 min, c) graph showing the increase of the temperature of the belt drive in time (on average by 0,94ºC/min)

a)

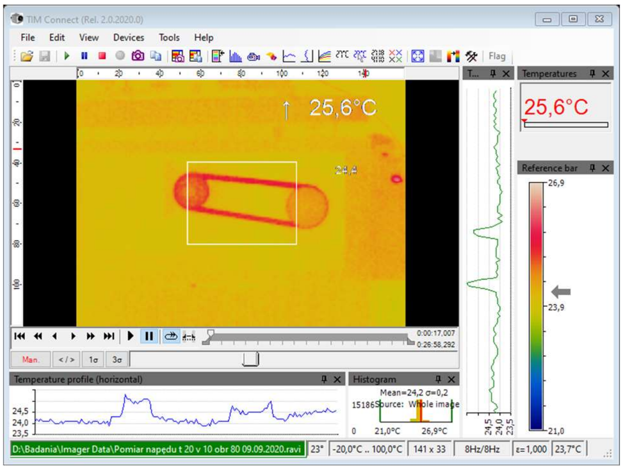

b)

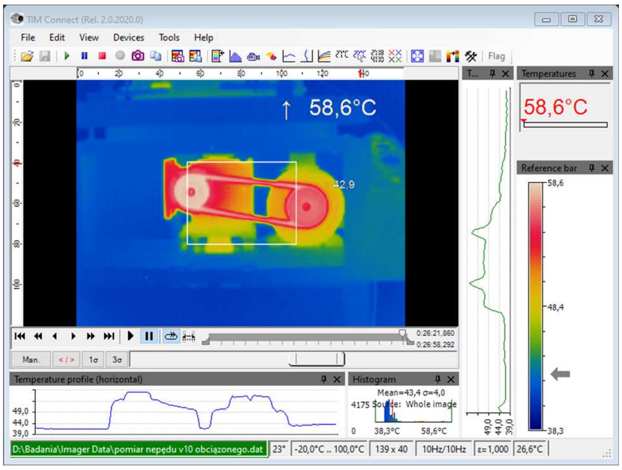

c)

Fig. 6. Results of the measurement of the temperature of the lapping machine drive system: a) in the initial moment, b) after 20 min of dressing the lapping disc with guiding rings (n_t = 80 min^{-1}) and manual refilling of the abrasive after 11.5 min, c) graph presenting the increase of the temperature of the belt drive in time

Results of the measurements of the temperature of the rotating lapping disc during idle mode can be seen in figures 7 and 8. When n_t = 40 min^{-1}, the highest temperature was noted in the centre of the lapping disc (it is thinner in this area) and it reached 27.6ºC. The average temperature in other areas on the surface of an active lapping disc was, on average, 24,5ºC. For n_t = 80 min^{-1} the increase of the tool temperature was, on average, 0.29ºC/min.

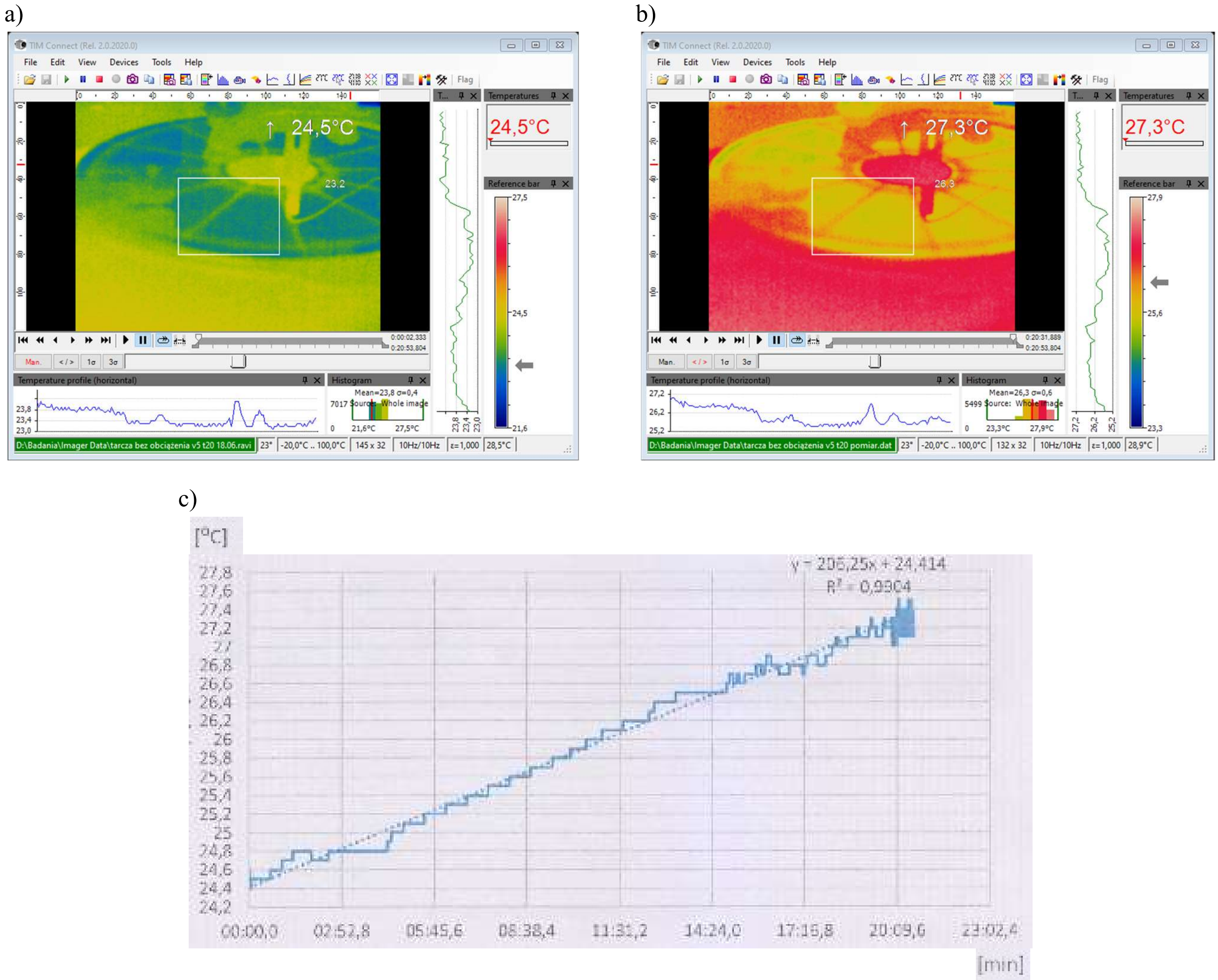

Fig. 7. Results of the measurements of the temperature of lapping disc in idle mode: a) in the initial moment, b) after 20 min (n_t = 40 min^{-1}), c) graph showing the increase of the temperature of the lapping disc in time (on average, 0.14ºC/min)

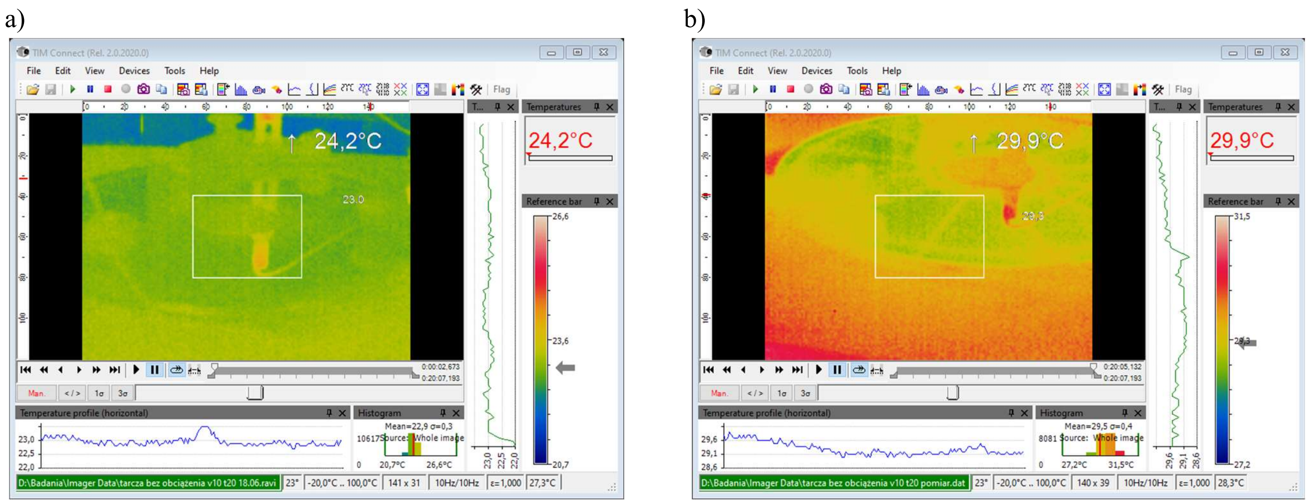

Fig. 8. Results of the measurements of the temperature of the lapping disc in idle mode: a) in the initial moment, b) after 20 minutes (n_t = 80 min^{-1})

3.3. Heating up of the actuating system of a machine during lapping of elements

The examinations of the increase of temperature of a single-disc lapping machine Abralap 380 were conducted during lapping of flat elements of C45 steel. The abrasive based on artificial corundum 95A F320 was dosed manually, with removed guiding rings. In the first stage, the machining was conducted throughout 10 minutes without refilling the abrasive. The rotational speed of the lapping disc was 80 min^{-1} (average lapping speed was 0.37 m/s), while unit pressure was 0.10 MPa. Figure 9 presents the example results of the temperature measurements. During the machining of a batch of elements, the average temperature of the tool increased to 33.4ºC, the temperature of the rollers guiding rings increased to 32.9ºC and the temperature of the guiding rings increased to 31.9ºC.

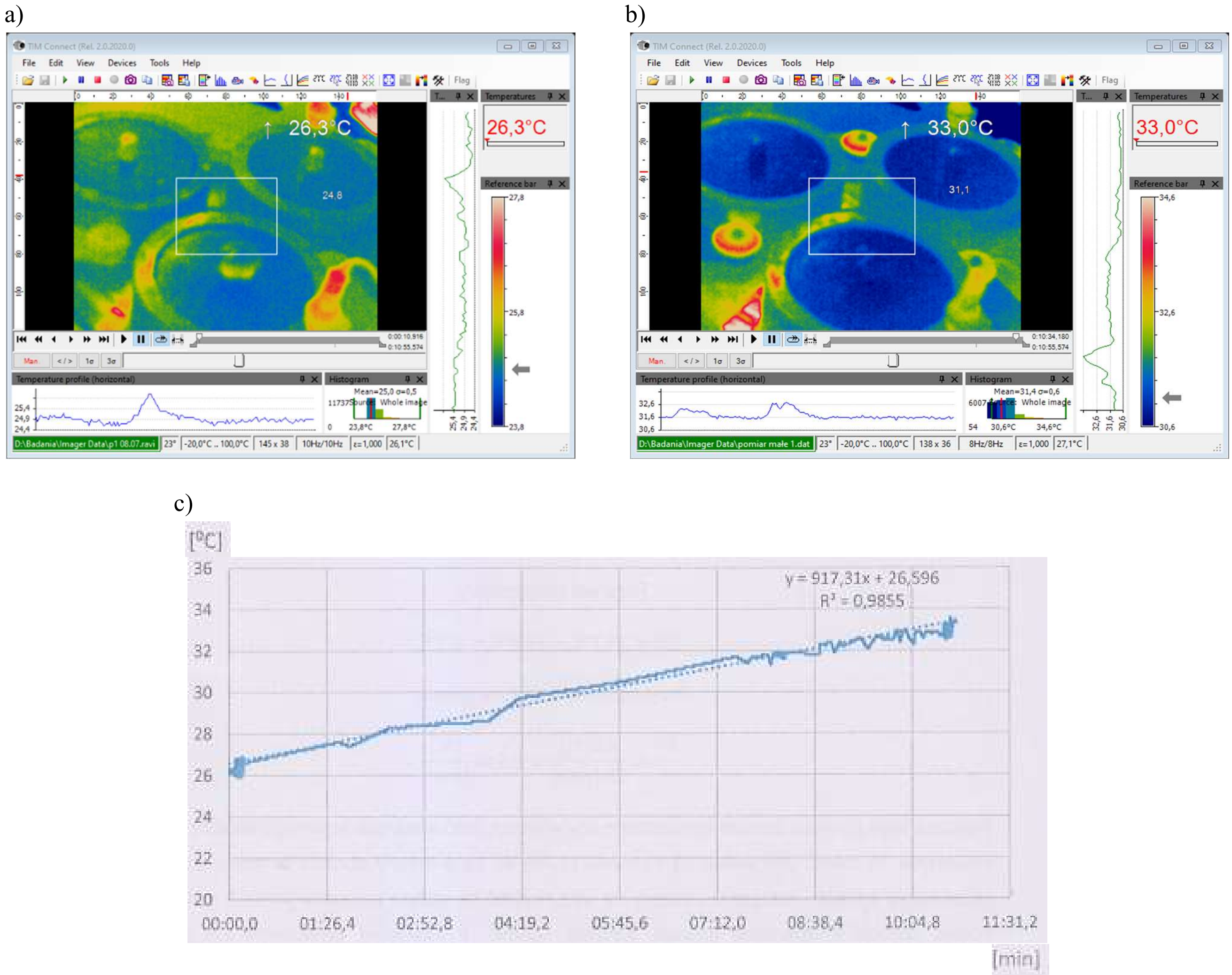

Fig. 9. Results of the measurements of the temperature of the actuating system during lapping of steel elements: a) in the initial moment, b) after 10 min (n_t = 80 min^{-1}), c) graph showing the increase of the temperature in time (on average by 0.67ºC/min)

When lapping duration was increased to 15 minutes, an increase of the average temperature of the lapping disc (fig. 10) occurred along with disturbances of the uniformity of rotational speed of the guiding rings and, consequently, separators with machined elements. With 5 minute long lapping (fig. 11), the intensity of the heating up of the tool was 0.12ºC/min.

A situation when the elements are lapped throughout 30 minutes, with refilling the abrasive after 15 minutes of machining is shown in fig. 12.

a) b)

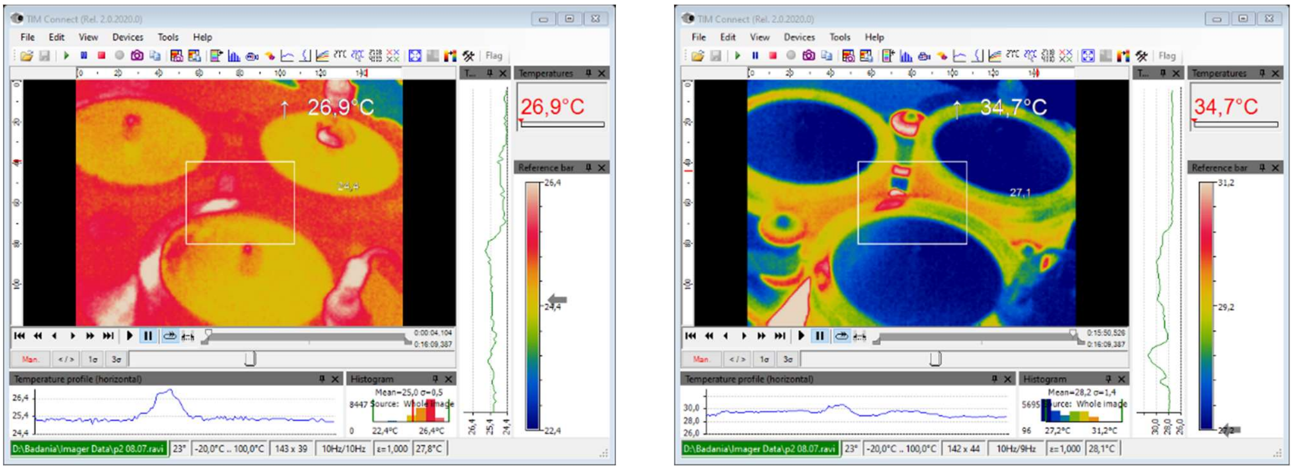

Fig. 10. Results of the measurements of the temperature of the actuating system of the lapping machine during lapping of steel elements: a) in the initial moment, b) after 15 minutes (n_t = 80 min^{-1})

a) b)

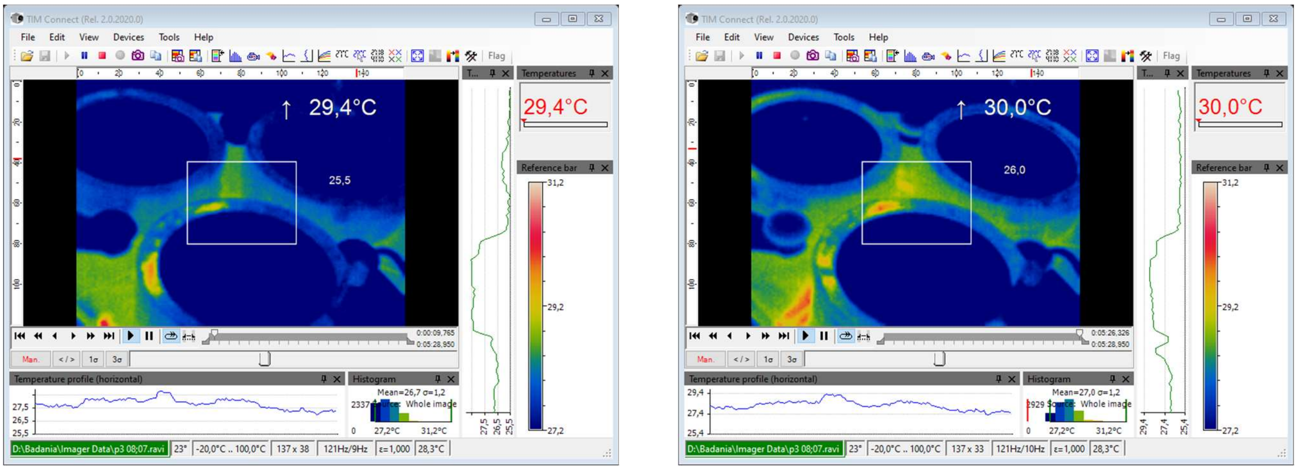

Fig. 11. Results of the measurements of the temperature of the actuating system during lapping of steel elements: a) in the initial moment, b) after 5 minutes (n_t = 80 min^{-1})

a) b) c)

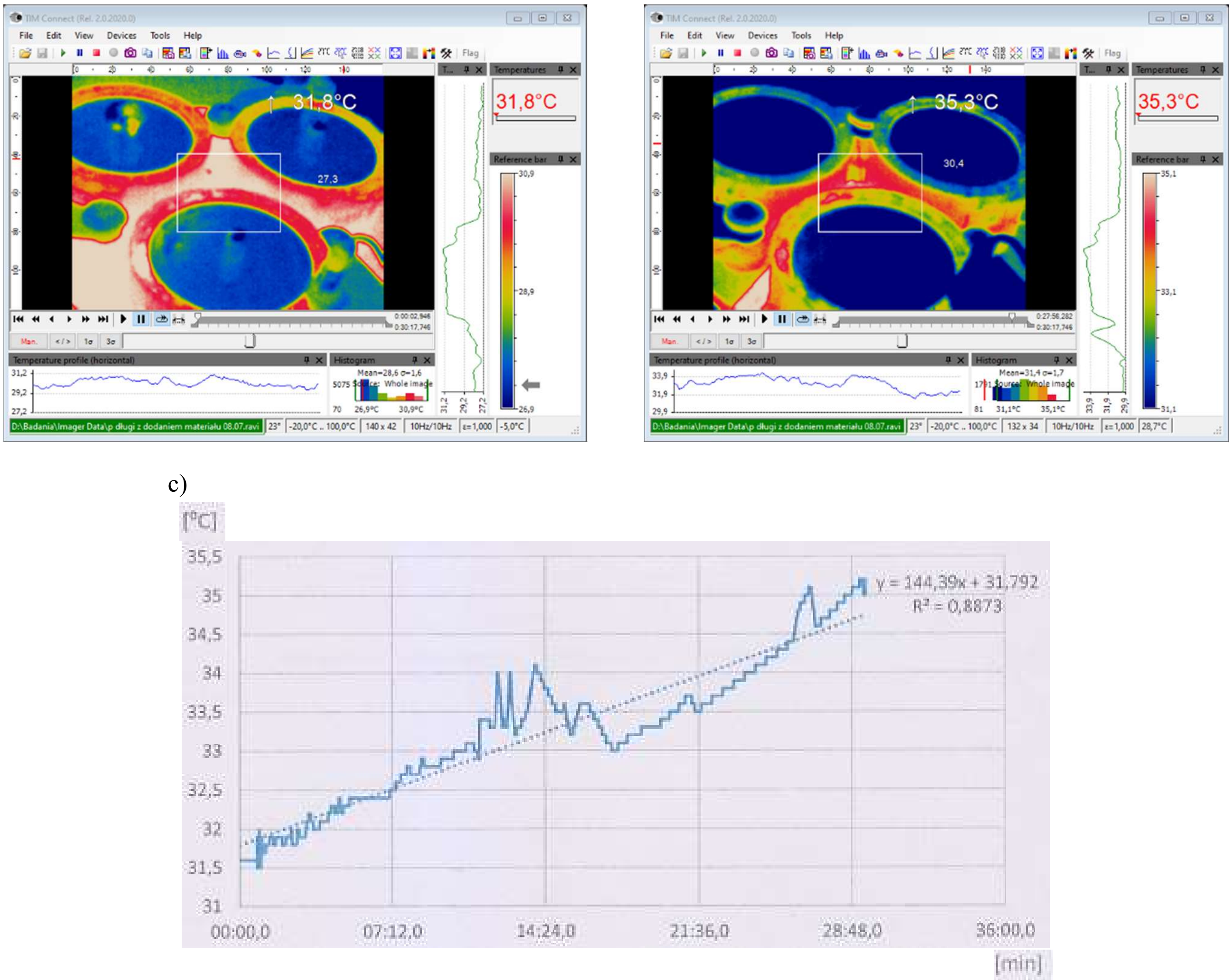

Fig. 12. Results of the measurements of the temperature of the actuating system during lapping of steel elements: a) in the initial moment, b) after 30 minutes (n_t = 80 min^{-1}), c) graph showing the increase of temperature in time

4. Summary

On the basis of the conducted examinations it can be seen that the assembly which exhibits the highest increase of temperature is the worm gear, being a part of the lapping machine drive system. Relatively approximate location of the gear and the lapping disc exerts a significant influence on the temperature of a metal tool. An important issue in construction of machines of such a type consists in the appropriate thermal insulation of the lapping disc.

Another significant factor consisted in the influence of the rotational speed of the lapping disc, and, consequently, of the guiding rings. In order to prevent the heating up of the elements of lapping machine drive system and of machined elements, one should aim at decreasing the values of kinematic parameters (lapping speed) and, obviously, decrease the exerted unit pressure. This will cause the prolongation of the time of main lapping of the elements, as well as the time of dressing the active surface of a tool. In opposite case, one should consider technological breaks between operations. If lapping technology is applied during the assembly of machine unit, the intensity of using the lapping machines does not have a significant meaning.

The increase of the temperature can also be limited by minimizing the ratio of filling the separators with lapped elements and, as it was shown in previous research, by applying a constant (drip or flood) dosage of the abrasive. If the nature of lapped materials requires the application of super-hard abrasives, i.e. expensive ones, it is possible to apply a forced water cooling system of the lapping disc.

Bibliography

1. Barylski A., Docieranie powierzchni płaskich w operacjach montażowych. Technologia i Automatyzacja Montażu. 2013, nr 3, s. 196-200.

2. Barylski A., Obróbka powierzchni płaskich na docierarkach. Wydawnictwo Politechniki Gdańskiej, Gdańsk 2013.
3. Bulsara V.H., Ahn Y., Chandrasekar S., Farris T.N., Polishing and lapping temperatures. Journal of Tribology, 1997, vol. 119. s. 163-170.
4. Horng J.H., Jeng Y.R., Chen C.L., A model for temperature rise of polishing process considering effects of polishing pad and abrasive. Transaction of ASME. 2004, vol. 126, s. 422-429.
5. Żabczyński P., Badania temperatury podczas docierania. Politechnika Gdańska, Wydział Mechaniczny. Praca dyplomowa, prowadz. pr. A. Barylski, Gdańsk 2020.

TECHNOLOGIA I AUTOMATYZACJA MONTAŻU ZESPOŁÓW • MASZYN • URZĄDZEŃ
TiAM kwartalnik naukowo-techniczny

Magdalena Dąbrowska[1], Daniel Medyński[2], Wiktor Bieliński[3], Krzysztof Kolbusz[4]

DOI: 10.7862/tiam.2022.3.4

REORGANIZATION OF THE ASSEMBLY STATION IN THE PRODUCTION PROCESS OF THE SLIDING FLOOR FOR RELOADING RAMPS IN THE CONTEXT OF IMPROVING THE QUALITY OF THE FINISHED PRODUCT

REORGANIZACJA STANOWISKA MONTAŻOWEGO W PROCESIE PRODUKCJI PODŁOGI PRZESUWNEJ DO RAMP PRZEŁADUNKOWYCH W KONTEKŚCIE POPRAWY JAKOŚCI GOTOWEGO PRODUKTU

Abstract

The paper presents the definitions of the term quality quoted in the literature on the subject. FMEA (*Failure Mode and Effects Analysis*) methodology was presented. A reloading ramp was characterized as the subject of the study. A cause-and-effect analysis of non-compliance in the finished product was performed using the Pareto-Lorenz diagram, Ishikawa diagram and brainstorming. The FMEA analysis of the assembly table indicated the elements of the workstation causing the most frequently occurring non-conformities. Based on the obtained results, corrective actions were proposed to reorganize the assembly station. The implemented activities made it possible to reduce the critical RPN coefficients for the elements of the assembly table and to shorten the time necessary to make one piece of the finished product.

Keywords: quality, production process, FMEA, assembly, Ishikawa diagram

Streszczenie

W artykule przedstawiono definicje pojęcia jakość przytaczane w literaturze przedmiotu. Zaprezentowano metodykę FMEA (*Failure Mode and Effects Analysis*). Scharakteryzowano rampę przeładunkową jako przedmiot badań. Dokonano analizy przyczynowo-skutkowej powstawania niezgodności w wyrobie gotowym z wykorzystaniem diagramu Pareto-Lorenza oraz diagramu Ishikawy i burzy mózgów. Dzięki przeprowadzonej analizie FMEA stołu montażowego wskazano elementy stanowiska powodujące najczęściej powstające niezgodności. Na podstawie uzyskanych wyników zaproponowano działania korygujące, mające na celu reorganizacje stanowiska montażu. Wdrożone działania naprawcze umożliwiły obniżenie krytycznych współczynników RPN w elementach stołu montażowego oraz skrócenie czasu niezbędnego do wykonania jednej sztuki wyrobu gotowego na stanowisku montażu.

Słowa kluczowe: jakość, proces produkcyjny, FMEA, montaż, diagram Ishikawy

1. Introduction

The activity of each economic entity, regardless of the surrounding reality, is inextricably linked with the need to bear the costs of good or bad quality, resulting from the implementation of the object of activity. To survive in highly competitive markets, companies must constantly improve the quality of their products or services, with a flexible approach to changing needs and shortening order fulfillment cycles.

Quality has been around mankind since ancient times. The first references can be found in the time of the Hammurabi Codex. In the literature on the subject, there are many definitions of the term quality [3, 5, 6, 16, 17, 20, 24, 27, 30, 34]. As emphasized by Schindler,

[1] PhD, Magdalena Dąbrowska, Collegium Witelona State University, Faculty of Technical and Economic Sciences, Department of Production Engineering and Logistics, Sejmowa Street 5A, 59-220 Legnica, Poland, e-mail: magdalena.dabrowska@collegiumwitelona.pl, ORCID: 0000-0002-9305-7123

[2] PhD Eng., Daniel Medyński, Collegium Witelona State University, Faculty of Technical and Economic Sciences, Department of Production Engineering and Logistics, Sejmowa Street 5A, 59-220 Legnica, Poland, e-mail: daniel.medynski@collegiumwitelona.pl

[3] Eng. Wiktor Bieliński, Collegium Witelona State University, Faculty of Technical and Economic Sciences, Research Club on Logistics and Transport.

[4] MSc, Eng. Krzysztof Kolbusz, Collegium Witelona State University, Faculty of Technical and Economic Sciences, Department of Production Engineering and Logistics, Sejmowa Street 5A, 59-220 Legnica, Poland, e-mail: krzysztof.kolbusz@collegiumwitelona.pl

Puls-Elvidge, Welzant and Crawford, defining the concept of quality is difficult because [37]:

- quality is an elusive term with many different interpretations depending on stakeholder views,
- quality is a multi-dimensional concept.

Taking into account the multidimensionality, Garvin distinguished five dimensions in which quality can be perceived. Among them there are [7]:

- absolute quality understood as the perfection of the product [36],
- product-related quality [25],
- quality relating to manufacturing [9],
- quality in relation to user requirements [4] ,
- quality in relation to value [1].

The same author proposed that the definitions of the concept of quality should be divided into seven categories. He distinguished the following categories of definitions: general, related to production, product, user, value creation, multi-dimensional and strategic [7].

According to the above-mentioned authors, when analyzing the definitions of the concept of quality, taking into account the level of product quality, three groups of definitions can be distinguished:

- definitions of quality in terms of utility, taking into account three approaches: economic, technical and identification,
- quality definitions in terms of cost, i.e. taking into account the cost of the manufactured product,
- definitions of quality in terms of meeting customer needs.

The authors recognize that quality is a common phenomenon, but it is difficult to clearly define the concept of quality. The problem of quality is complex. It can be analyzed not only technically or economically, but also socially, philosophically or psychologically.

Manufacturing companies operating in the present conditions are forced to constantly improve their production processes and ensure the quality level of products in line with customer expectations. Many methods and quality management tools are used to carry out the cause-and-effect analysis, including: Ishikawa diagram (more on Ishikawa diagram see [13, 14, 18]), 8D method (more on 8D method see [12, 22, 23]) or FMEA analysis.

In the literature, there are descriptions about the issues which can be found on the assembly station [15, 19, 21, 28, 32].

The aim of this work is to reorganize the assembly station in the production process in terms of improving the quality of the finished product and reducing assembly time. As an example, the production of a sliding floor for docking stations was selected. The selection of the assembly station in the discussed production process was dictated by the analysis of non-compliance of finished products and the determination of the reasons for their formation. The evaluation of the proposed reorganization solutions was made on the basis of the FMEA method.

2. FMEA methodology

FMEA (Failure Mode and Effects Analysis) analyzes the cause-and-effect relationships of potential defects, taking into account the risk factor, and allows for earlier implementation of corrective actions to counteract failures, errors and their effects [10]. This method was initially used in the United States in the 1960s. The analysis was developed and used for the first time by NASA in space flight projects. Despite its success, this method was not used by other industries until the 1970s. In the early 1980s, US automotive companies formally introduced FMEA analysis to their product development processes [2, 26].

In the literature on the subject, two types of FMEA analyzes are most often distinguished: product analysis (D-FMEA) and process analysis (P-FMEA) [31, 33]. Process FMEA is used in processes that are difficult to control, in the planning phase of technological processes and service processes, in order to improve processes that do not provide the required performance [39].

The procedure of designing the FMEA analysis has been presented, among others, in the studies [26, 33, 35]. It consists of the following steps:

- creation of the FMEA team,
- description of the product, process that will be analyzed,
- creating a block diagram showing the main components (product FMEA) or process steps (process FMEA),
- creating a list of potential failures, their causes and impact on the product or process,
- assigning coefficients (Severity, Occurrence, Detection) for each non-compliance,
- RPN (Risk Priority Number) calculation according to the formula (RPN = Severity X Occurrence X Detection),
- development of a recovery plan,
- taking corrective actions,
- recalculation of RPN after implementation of corrective actions,
- comparison of RPN before and after implementation of corrective actions and reassessment of potential non-conformities.

FMEA analysis is used for [38]:

- systematic identification of possible product / process non-conformities,
- testing the probability of errors in the manufacturing or assembly process,
- elimination of non-compliance or minimization of the related risk,
- interpretation of factors that may affect the stability of the production process,
- searching for solutions to existing problems,
- indication of areas requiring increased supervision,
- audit planning.

3. Characteristics of a reloading ramp

Reloading ramps enable a direct connection of the delivery vehicle with the warehouse surface, which enables a forklift to enter the vehicle's load box. The loading ramp is equipped with a system that enables automatic adjustment of the ramp level to the vehicle floor. By using this tool, loading and unloading of a given product is performed only on a horizontal plane.

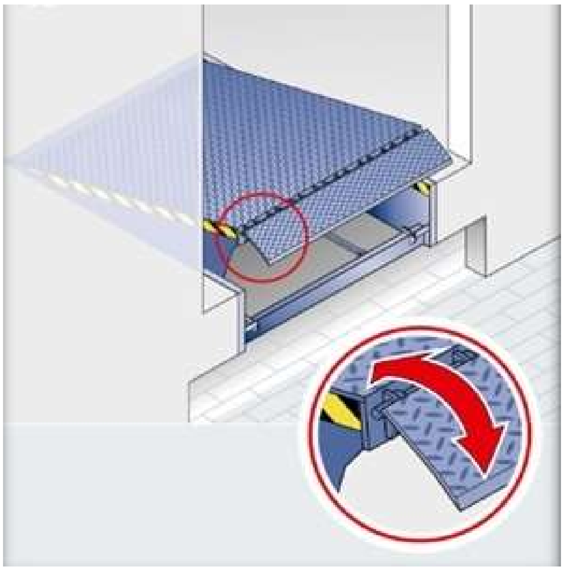

Fig. 1. Reloading ramp with a folding floor

Two types of ramps are manufactured in the examined enterprise. The principle of their operation and construction differ from each other only in the method of mounting the extendable platform (flap), which is a link between the ramp platform and the car loading surface. Both types of ramps consist of three basic elements: platform, tear plate and ribs stiffening the structure. The loading ramps are also equipped with frames, platforms, wheel guides and buffers (bumpers). The structure of the ramp with a sliding floor consists of interlocking beams of the platform, an extendable flap and side guide profiles (Fig. 1, Fig. 2). All loading ramps are manufactured in accordance with the provisions of the PN EN 1398 standard, and their size is appropriately adapted to the assumed load capacity.

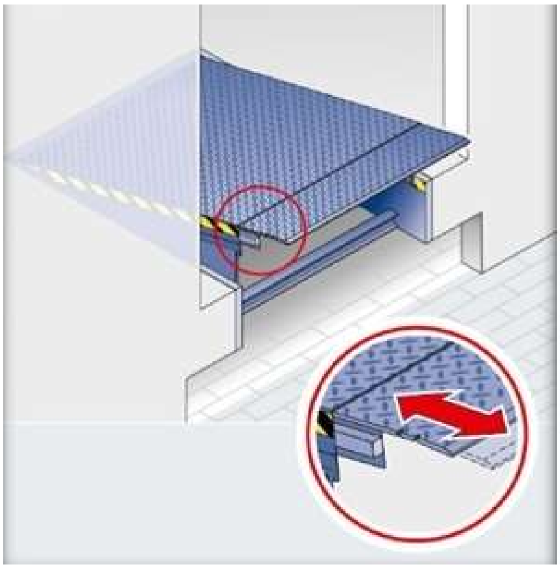

Fig. 2. Reloading ramp with a sliding floor

The time necessary to make one piece of the finished product at the assembly station is 45 minutes.

4. Cause-and-effect analysis of non-compliance in the finished product

The quantitative analysis was carried out in relation to products manufactured in one quarter. In the analyzed period 1250 units of a retractable platform for the loading ramp were manufactured. Based on internal complaints, 126 non-conformities were identified. Seven types of product non-compliance were noted. They included:

- D1 - incorrectly welded ribs,
- D2 - incorrectly welded beam,
- D3 - incorrectly positioned ribs,
- D4 - beam angle not maintained,
- D5 - folded ribs,
- D6 - scratches and surface crushing,
- D7 - unpainted surface.

Table 1 presents the defects in descending order with their percentage share calculated and cumulative values. This allowed the identification of a small number of defects that cause the most severe consequences. The most important problems in quality of finished products are:

- incorrectly welded ribs, which cause almost 35% of all defects,
- incorrectly welded beam, which cause almost 20% of all defects,

- incorrectly positioned ribs, which cause almost 13% of all defects,
- beam angle not maintained, which cause about 9,5% of all defects,
- folded ribs, which cause more than 8,5% of all defects,
- scratches and surface crushing, which cause almost 8% of all defects,
- unpainted surface, which cause more than 6% of all defects.

Based on the identified and sorted inconsistencies in Table 1, the Pareto-Lorenz diagram was prepared (Fig. 3). Two defects (D1 - incorrectly welded ribs, D2 - incorrectly welded beam) cause more than 50% of all defects. Four defects (D1 - incorrectly welded ribs, D2 - incorrectly welded beam, D3 - incorrectly positioned ribs, D4 - beam angle not maintained) result in more than 75% of all defects.

Table 1. Defects in the tested product

No defect	Type of defect	*Frequency* for 1250 pcs.	*Frequency* [%]	*Cumulative frequency*	*Cumulative frequency* [%]
D1.	Incorrectly welded ribs	44	34,92	44	34,92
D2.	Incorrectly welded beam	25	19,84	69	54,76
D3.	Incorrectly positioned ribs	16	12,70	85	67,46
D4.	Beam angle not maintained	12	9,52	97	75,98
D5.	Folded ribs	11	8,73	108	85,71
D6.	Scratches and surface crushing	10	7,94	118	93,65
D7.	Unpainted surface	8	6,35	126	100,00

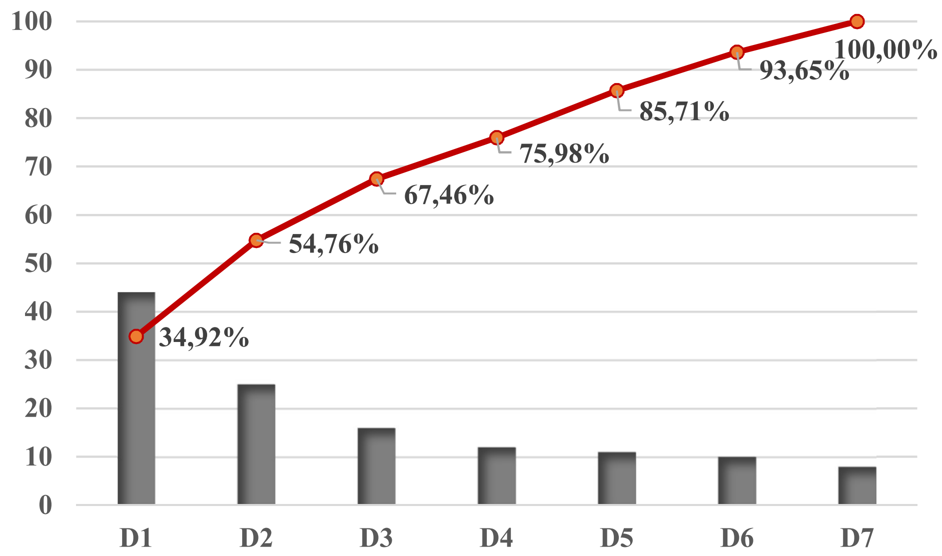

Fig. 3. Pareto-Lorenz diagram

For three inconsistencies, constituting nearly 70% of all inconsistencies, an analysis of the causes of inconsistencies was performed using the Ishikawa diagram. The main analyzed areas are described, among others, in [11]. Fig. 4 shows the Ishikawa diagram indicating the causes of the most common defect "incorrectly welded ribs". Determining the causes of non-compliance was possible thanks to brainstorming and observations of the assembly station employees. The cause-and-effect analysis has shown that the main cause of the incorrectly welded ribs lies in the construction of the assembly table.

While welding the ribs, workers have trouble keeping the ribs in the correct position, which results in incorrect welding. In the case of two consecutive irregularities, i.e. "incorrectly welded beam" and "incorrectly positioned ribs", the construction of the assembly table was also indicated as the main cause of the non-compliance.

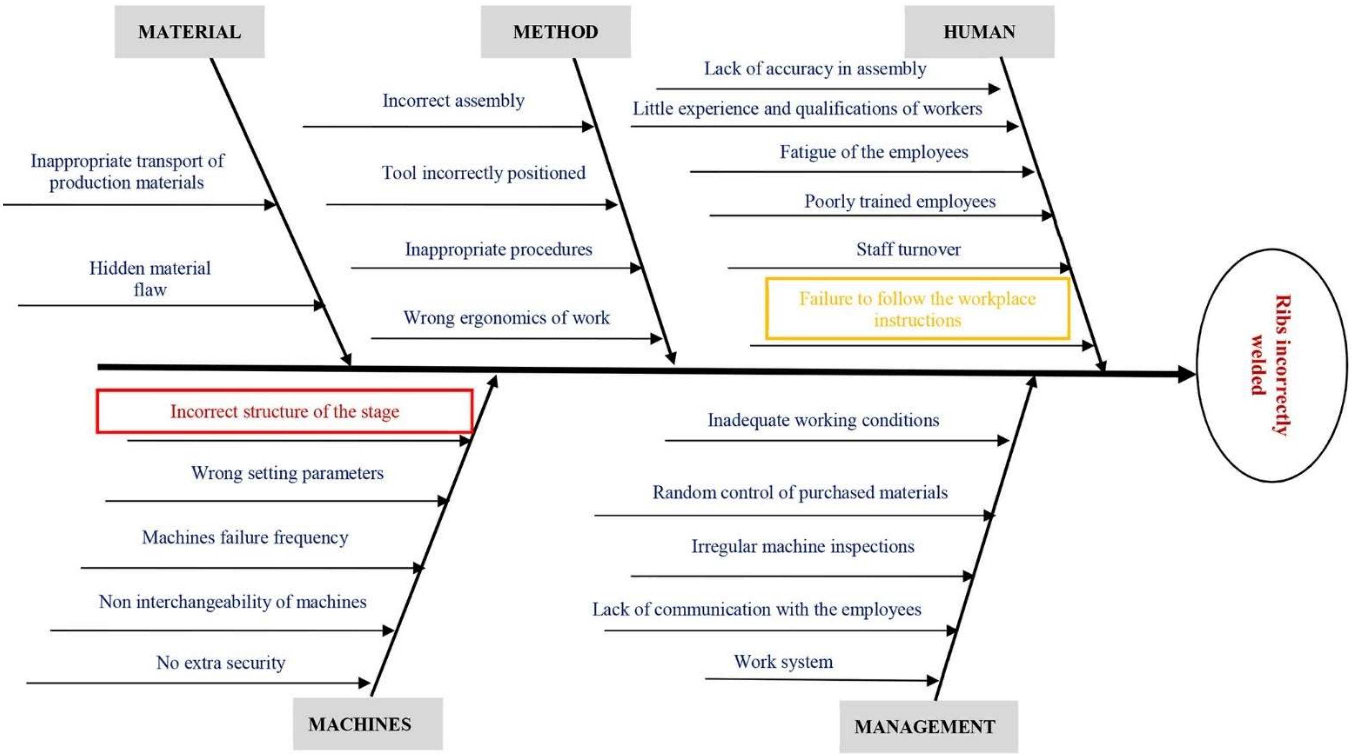

Fig. 4. Ishikawa diagram showing the causes of the "incorrectly welded ribs" defects

5. Reorganization of the assembly station - FMEA analysis

The most important incompatibilities of the finished product include: improperly welded ribs, improperly welded beam and improperly positioned ribs. The incorrect structure of the assembly table was indicated as the main cause of the defects.

The assembly table consists of the following elements (Fig. 5):

- rear strip,
- a pressure beam, which includes a lug fixing the position of the ribs, a movable beam and a ruler,
- hydraulic system,
- control system,
- table top for assembly, consisting of the rear beam guide, table legs and a roller for ejecting ready-made elements.

The rear strip is responsible for pressing the beam and setting the beam position. The task of the clamping beam is to maintain the rib angle and to press the rib against the platform (lug fixing the position of the ribs), and also to measure the distance of the ribs (ruler). The tasks of the hydraulic system include pressing the main beam, and the control system monitoring the hydraulic cylinders. The table top for assembly is a place for storing and welding the platform.

Based on conversations with the employees of the assembly station and own observations, a list of the elements of the assembly table responsible for resulting in the causes and effects of non-compliance in the finished product was created. In the next step, the RPN, i.e. Risk Priority Number, was calculated (Table 2).

The conducted FMEA analysis of the assembly table showed five most important defects (the RPN coefficient exceeds the value of 100, which is considered a critical value in the examined company), which affect the incorrect course of the assembly process. The irregularities concerned such elements as: the rear strip, the paw fixing the position of the ribs and the top of the stage. Considering the number of incompatibilities in the finished product, it should be noted that:

- the cause of an incorrectly welded rib is the lack of pressing force on the internal ribs, which affects the fact that the ribs do not have a right angle during the assembly process,

- the cause of an incorrectly welded beam is improper structure of the beam, in which there are bolts, which while pressing the beam move the beam away from the platform,
- the cause of improperly positioned ribs is the curved surface of the assembly table, which causes the platform to bend.

Based on the obtained results, a repair plan was developed taking into account the structural changes of the assembly station, corrective actions were implemented, and then the RPN coefficient was recalculated (Table 3). The repair plan for the construction of the assembly table included the following actions:

- the use of a bar clamping the beam with a chain,
- the use of an electromagnet,
- changing the structure of the rib paw,
- placing a pneumatic actuator on each foot,
- use of thicker material for the table top - introduction of a strengthening frame.

The time necessary to make one piece of the finished product at the assembly station after implementing corrective actions was 30 minutes. Table 4 shows the results of the FMEA analysis of the stage before and after the implementation of corrective actions.

Fig. 5. Assembly table

Table 2. FMEA analysis for the assembly table

Assembly table element	Cause of defect	Consequences of a defect	RPN			
			R	P	N	RPN
Rear strip	Incorrect construction of the rear strip	Beam incorrectly welded	7	3	6	**126**
	Moving beam	Beam angle not maintained	6	3	6	**108**
Paw fixing the position of the ribs	Wrong paw construction	Wrinkled rib	8	2	7	**112**
	No downforce on the inner ribs	Rib badly welded	7	3	7	**147**
Ruler	Unreadable reading from the ruler	Ribs incorrectly positioned	3	2	8	48
Hydraulic system	Broken serpent	No oil pressure	3	2	4	24
	Damaged actuator	Actuator not working	3	3	5	45
Control system	Damage to electrical wires	No actuator reaction	2	6	8	96
Table top for assembly	The curve of the table surface - dents and unevenness	Ribs incorrectly positioned	6	3	7	**126**

Table 3. FMEA analysis for the assembly table after the implementation of corrective actions

Assembly table element	Cause of defect	Efforts to improve	RPN			
			R	P	N	RPN
Rear strip	Incorrect construction of the strip	The use of a bar clamping the beam with a chain	5	3	6	**90**
	Moving beam	The use of an electromagnet	1	3	6	**18**
Paw fixing the position of the ribs	Wrong paw construction	Change in the structure of the rib paw	2	2	7	**28**
	No downforce on the inner ribs	Pneumatic actuator is placed on each foot	3	3	7	**63**
Assembly table top	The curve of the table surface - dents and unevenness	The use of a thicker table top and the introduction of a rein-forcing frame	5	2	7	**70**

Table 4. Assembly table FMEA analysis results before and after the implementation of corrective actions

Assembly table element	Task	RPN before modernizing the assembly table				RPN after modernization of the assembly table			
		R	P	N	RPN	R	P	N	RPN
Rear strip	Pressing down the beam	7	3	6	**126**	5	3	6	**90**
	Setting the position of the beam	6	3	6	**108**	1	3	6	**18**
Paw fixing the posi-tion of the ribs	Maintaining the rib angle	8	2	7	**112**	2	2	7	**28**
	Pressing the rib to the platform	7	3	7	**147**	3	3	7	**63**
Assembly table top	Assembly and welding of the platform	6	3	7	**126**	5	2	7	**70**

6. Summary

The aim of the work was to reorganize the assembly station in the production process in terms of improving the quality of the finished product and reducing the assembly time. Based on the conducted analyzes, it can be concluded that:

- the Pareto-Lorenz analysis showed that the incidence of "incorrectly welded ribs" was 34.92%, "improperly welded beam" - 19.84%, and "incorrectly positioned ribs" - 12.70%,
- analysis of the Ishikawa diagram and brain-storming indicated that the most common causes of non-compliance are: incorrect con-struction of the assembly table, non-compliance with workplace instructions, improper ergono-mics of work and lack of communication with employees,
- the FMEA analysis of the assembly table showed that the elements of the station causing the most frequently occurring non-conformities are: the back strip, the clamp fixing the position of the ribs and the top of the assembly table,
- on the basis of the FMEA analysis of the assembly table, in relation to the critical causes of non-compliance, the following corrective actions were proposed: the use of a bar clamping the beam with a chain, the use of an electro-magnet, changing the structure of the rib paw, placing a pneumatic actuator on each paw, as well as using a thicker table top and the introduction of a strengthening frame,
- corrective actions reduced the critical RPN coefficients in the elements of the assembly table and shortened the time necessary to make one piece of the finished product at the assembly station from 45 minutes to 30 minutes.

Literature

1. Broh R.A. (1982). Managing quality for higher profits: A guide for business executives and quality managers. New York: McGraw-Hill.
2. Ćatić D., Arsovski S. (2011). *FMEA in product development phase.* "Kragujevac: 5th International Quality Conference": pp. 679-686.
3. Crosby P.B. (1979). *Quality is Free.* New York: McGraw-Hll Book Co.

4. Deming W.E. (1982). *Quality, productivity and competitive position*. Cambridge: Center for Advanced Engineering Study, MIT.
5. Deming W.E. (1988). *Out of the Crisis.* Camlbridge, MA: Massachusetts Institute of Technology, Center for Advanced Engineering Study.
6. Feigenbaumn A.V. (1983). *Total Quality Control*, 3ed edition, New York: McGraw-Hill Book Co.
7. Garvin D.A. (1984). "Sloan management review". *What does product quality really mean*, 25: 25-43.
8. Garvin D.A. (1988). *Managing Quality*, New York: The Free Press.
9. Gilmore H.L. (1974). "Quality Progress". *Product conformance cost*, no. 7(5): 16-19.
10. Ginn D.M., Jones D.V., Rahnejat H., Zairi M. (1998). "European Journal of Innovation Management". *The "qfd/fmea interface*, Vol. 1, No. 1: 7– 20.
11. Górny A. (2013). *The use of Ishikawa diagram in occupational accidents analysis*, in: *Occupational Safety and Hygiene (SHO 2013),* Arezes P., Baptista J.S., Barroso M.P., Carreiro P., Cordeiro P., Costa N., Melo R., Miguel A.S., Prestrelo G. (eds.): pp. 162-163.
12. Grecu I., Belu N., Misztal A. (2015). "International Conference on Management and Industrial Engineering". *Increasing customer satisfaction through the application of the 8d methodology*, No. 7: 488-495.
13. Gwiazda A. (2006). "Journal of Achievements in Material and Manufacturing Engineering". *Quality tools in a process of technical project management*, 18: 328-343.
14. Hagemeyer C., Gershenson J., Johnson D. (2006). "The TQM Magazine". *Classification and application of problem solving quality tools: A manufacturing case study*, 18: 455-483.
15. Hanson R., Medbo L., Medbo P. (2012). Journal of Manufacturing Technology Management". *Assembly station design: a quantitative comparison of the effects of kitting and continuous supply*, Vol. 23 No. 3, 315-327.
16. Hoyer R.W., Hoyer B.B., Crosby P.B., Deming W.E. (2001). "Quality Progress". *What is quality*, 34(7): 53-62.
17. Ishikawa K. (1985), *What is Total Quality Control? The Japanese Way*. Englewood Cliffs, NJ: Prentice-Hall Inc.
18. Ismyrlis V. (2017), "The TQM Journal". *The contribution of quality tools and integration of quality management systems to the organization*, 29: 677-689.
19. Jiang Q., Yan Z. (2022), *Optimal Design of Intelligent Production Line Based on Single-Station Assembly.* In *Proceedings of the Eighth Asia International Symposium on Mechatronics.* Springer, Singapore, 802-812.
20. Juran J.M., Godfrey A.B. (ed.) (2003), *Juran's quality handbook*. 5th edition, New York: McGraw-Hill.
21. Kamble R., Kulkarni V. (2014), "International Journal of Research in Engineering and Technology". *Productivity improvement at assembly station using work study techniques* , 3(09): 480-487
22. Kaplík P., Prístavka M., Bujna M., Viderňan J. (2013). "Advanced Materials Research". *Use of 8D method to solve problems*. vol. 801: 95-101.
23. Krajnc M. (2012). "Journal of Universal Excellence". *With 8D method to excellent quality*, *3*(10): 118-129.
24. Kumar P., Raju N.V.S., Kumar M.V. (2016). "International Journal of Scientific Engineering and Technology". *Quality of quality definitions-an analysis*, 5(3): 142-148.
25. Leffler K.B. (1982). "The American Economic Review". *Ambiguous changes in product quality*, 72(5): 956-967.
26. Mikulak R.J., McDermott R., Beauregard M. (2017). *The basics of FMEA*. Boca Raton: CRC press.
27. Oakland J.S. (1995). *Total Quality Management text with cases*. Oxford: Butterworth-Heinemann.
28. Pattison A. (2006). *Operator-centric assembly station design*, doctoral dissertation, Loughborough University.
29. Pirsig R.M. (1974). *Zen and the Art of Motorcycle Maintenance.* New York: William Morrow & Co.
30. Reeves C.A., Bednar D.A. (1994). "Academy of management Review". *Defining quality: alternatives and implications*, 19(3): 419-445.
31. Sharma K.D., Srivastava S. (2018). "Journal of Advance Research in Aeronautics and Space Science". *Failure mode and effect analysis (FMEA) implementation: a literature review*, vol. 5:1-17.
32. Singh S.N., Rajesh K.R., Sunil S. (2022). "Materials Today: Proceedings". *Ergonomics control–Assembly station,* 54: 513-518.
33. Stamais D.H. (2003). *Failure Mode and Effect Analysis. FMEA from Theory to Execution*. Milwaukee: ASQ Quality Press.
34. Taguchi G., Wu Y. (1979). *Introduction to Offline Qutality Control*. Negaya: Central Japan Quality Control Association.
35. Teng S.H.G., Ho S.Y.M. (1996). "International Journal of Quality & Reliability Management". *Failure mode and effects analysis: an integrated approach for product design and process control*, 13(5): 8-26.
36. Tuchman B.W. (1980). "New York Times Magazine". *The decline of quality*, 2(104): 38-41.
37. Welzant H., Schindler L., Puls-Elvidge S., Crawford L. (2011). "Higher Learning Research Communications". *Definitions of quality in higher education: A synthesis of the literature*, 5(3): 3-13.
38. Wu Z., Liu W., Nie W. (2021). "The International Journal of Advanced Manufacturing Technology". *Literature review and prospect of the development and application of FMEA in manufacturing industry*, 112(5): 1409-1436.
39. Yang C.S., Zou Y.N., Lai P.H., Jiang N. (2015). "Applied Intelligence". *Data mining-based methods for fault isolation with validated FMEA model ranking*, vol. 43, iss. 4: 913-9

TiAM kwartalnik naukowo-techniczny
TECHNOLOGIA I AUTOMATYZACJA MONTAŻU
ZESPOŁÓW • MASZYN • URZĄDZEŃ

Jacek Domińczuk[1], Małgorzata Gałat[2]

DOI: 10.7862/tiam.2022.3.5

DESIGN SOLUTION FOR AUTOMATED INSTALLATION SYSTEM OF WASHERS ON FIXING PINS

ROZWIĄZANIE KONSTRUKCYJNE ZAUTOMATYZOWANEGO SYSTEMU MONTAŻU PODKŁADEK NA KOŁKACH USTALAJĄCYCH

Abstract

The article presents a design solution for a tool for the automatic release and assembly of washers on ISO pins in order to prevent a heating mat from moving during tank forming. This solution minimizes the risk that washers get displaced. It also ensures safe and controlled release of washers without the assembly process.

Keywords: automation, assembly, control

Streszczenie

W artykule przedstawiono rozwiązanie konstrukcyjne urządzenia służącego do zautomatyzowanego wydawania i montażu podkładek na kołkach ustalających w celu zabezpieczenia maty grzejnej przed przesunięciem w trakcie procesu formowania zbiornika. Rozwiązanie to minimalizuje ryzyko obecności podkładek poza miejscami do tego przeznaczonymi. Zapewnia również możliwość bezpiecznego kontrolowanego wydania podkładek bez realizacji montażu.

Słowa kluczowe: automatyzacja, montaż, kontrola

1. Introduction

There is a growing tendency for various manufacturing companies manufacturing to automate basic, auxiliary and service processes. This trend can also be observed with respect to assembly processes, though, undoubtedly, the advancement of automatic system implementation in assembly processes is not yet as intense as in other manufacturing processes. There are many reasons for that, the most important being [6]:

- increased design and functional complexity of various electromechanical products, the assembly of which would require special, expensive and often unreliable devices,
- limited possibility of series production, which makes it unprofitable to implement automatic assembly devices,
- great diversity of product types (e.g. standard, modular and functional), which requires considerable flexibility of automatic assembly devices,
- insufficient manufacturability of product design due to automated assembly requirements,
- lack of series production of typical modules for automatic assembly that would allow easy configuration of automatic assembly devices depending on the assembly need,
- necessity to produce specialized assembly units dedicated for a specific use.

Despite the above-mentioned factors that limit the use of automated systems in machine assembly, such systems are gradually becoming more and more popular, thus contributing to repeatability and automatic control of the assembly process.

A technological process can be automated if operations performed in this process are mechanized. Mechanization means that physical human work is replaced with machine work. To achieve it, it is

[1] PhD, Eng. Jacek Domińczuk, Lublin University of Technology, Faculty of Mechanical Engineering, Katedra Automatyzacji i Informatyzacji Produkcji, 20-618 Lublin, ul. Nadbystrzycka 36, tel. 81 5384585; fax: 81 5384496, e-mail: j.dominczuk@pollub.pl, ORCID: 0000-0003-2536-5340.
[2] MSc. Eng. Małgorzata Gałat, Centrum Energooszczędnych Rozwiązań, www.e-cer.pl. 20-468 Lublin, ul. Energetyków 17, tel. +48 667306767, e-mail: m.galat@e-cer.pl.

necessary to use proper mechanical devices which will work under human supervision. One can distinguish four basic groups of driving elements: mechanical, pneumatic, electric and hydraulic. Following mechanization, the process can be automated so that the machines perform planned operations either without or with limited human participation [2]. This is possible thanks to the use of control systems such as programmable microprocessor controllers.

The most frequent reasons for assembly automation include:

- the limitation of production capacity in defined assembly operations, which makes it impossible to fully use the technological possibilities of other mechanized and partially automated manufacturing techniques on a manufacturing line,
- the necessity to ensure that a given process can be completed within a defined time, which forces the need for process automation [1],
- the need to offer competitive solutions that reduce the probability of manufacturing faulty products.

Such situations create opportunities for the companies specializing in the design and manufacture of semi-automated and automated assembly machines, as well as for the suppliers producing components for these machines.

According to the opinion of the author of [6], in order to make the most of opportunities which increase during the times of economic prosperity and diminish in a crisis period, it is necessary to:

- have experienced, creative and innovative team of designers able to promptly solve complex problems,
- have proper information systems supporting designers works, activities of planners implementing these projects (supplying, prioritizing and ordering tasks, using production capacities and resources, etc.),
- have proper technical infrastructure enabling fast and qualitative implementation of projects and have good connections with suppliers, co-operators and sub-contractors facilitating performance of these works.

The need for creativity results mainly from the fact that assembly automation does not always reflect operations that are performed manually. In such situations, problems must be solved in an innovative way, one that guarantees high efficiency, stable quality, work safety, and functional reliability of the automated assembly system.

To meet the above requirements, it is necessary to conduct basic, applied and development research [4, 5]. The aim of these research efforts is to elaborate and propose various solutions, methods, tools, instruments as well as other elements for effective and reliable process automation.

2. Project requirements

The project task included building a station for an automated assembly of washers for attaching a mat to fixing pins. Dimensions of the mat are presented in Fig. 1. The mat is made of high-density polyethylene (PE-HD).

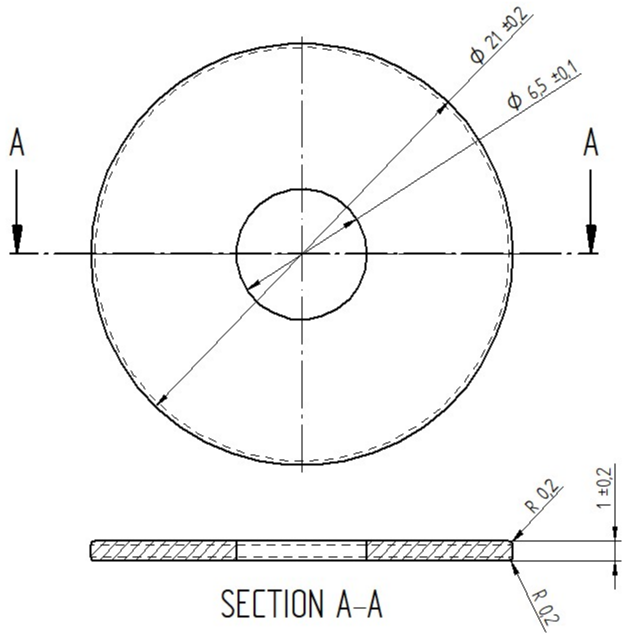

Fig. 1. Dimensioned drawing of a securing washer

Dimensions of the fixing pin are presented in Fig. 2.

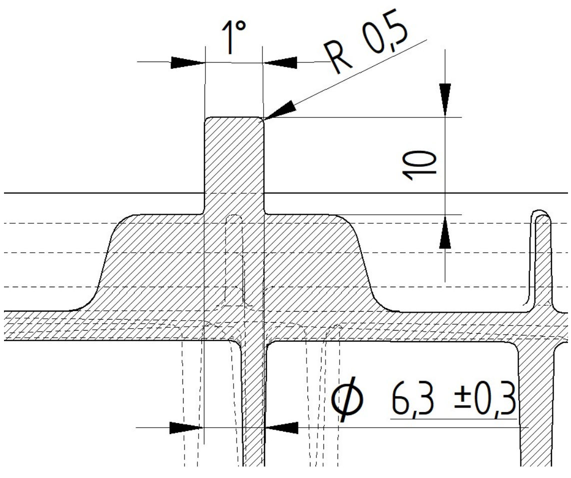

Fig. 2. Dimensions of an fixing pin

The washer is automatically assembled on the pin after putting the mat on. The operator sets an assembling head on the assemble position, and after detecting the proper setting the device assembles the washer automatically. Fig. 3 presents the status of the product before and after assembling the protection (washer).

The number of released washers is automatically defined based on product identification. The device is equipped with a storage of washers in the amount enabling to assemble a full set of washers for one product (max. 13 pieces), without the need to refill it. The storage is refilled when the product is exchanged in a work nest. The washers are added to the main hopper automatically from a tray located at the height of the working table. Product is identified based on a barcode placed thereon.

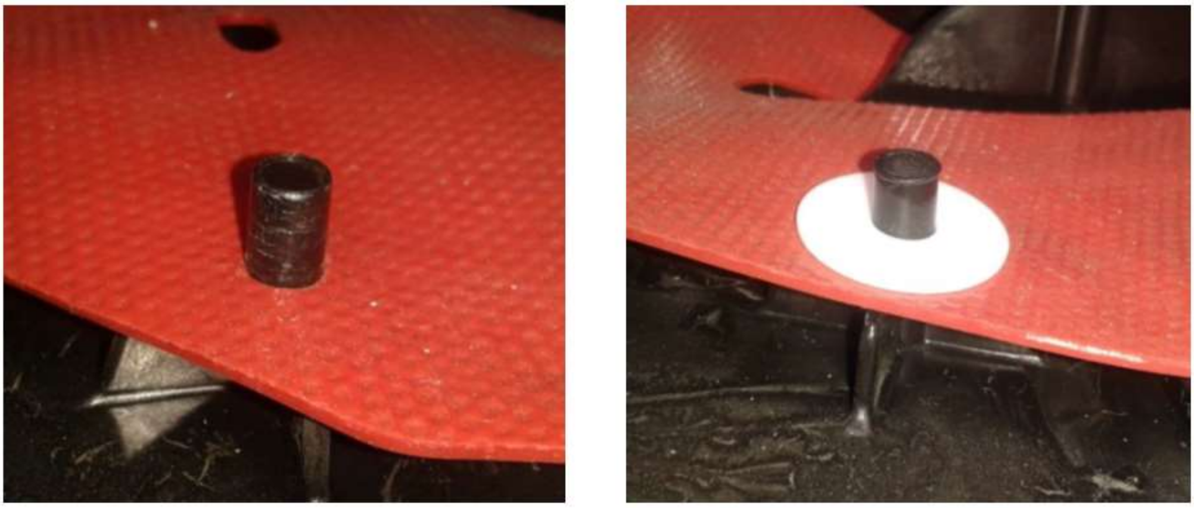

Fig. 3. Product before and after protection assembly

A simplified view of the product with assembled washers is shown in Fig. 4.

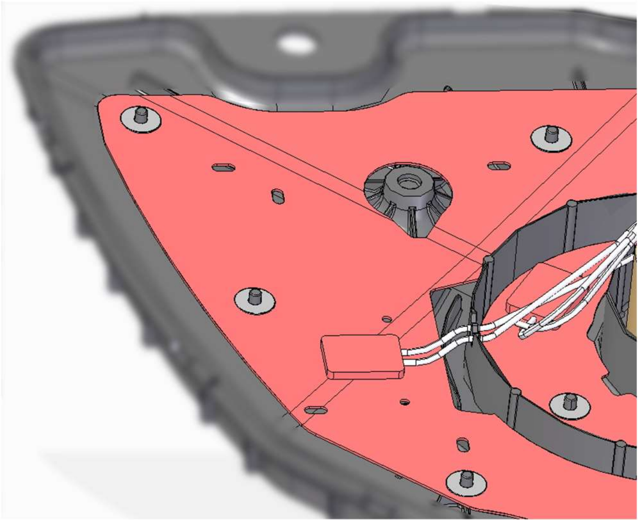

Fig. 4. Simplified view of a product with assembled washers

3. Technical solutions

Based on the presented requirements, a technological solution for a washer assembly station was devised (Fig. 5).

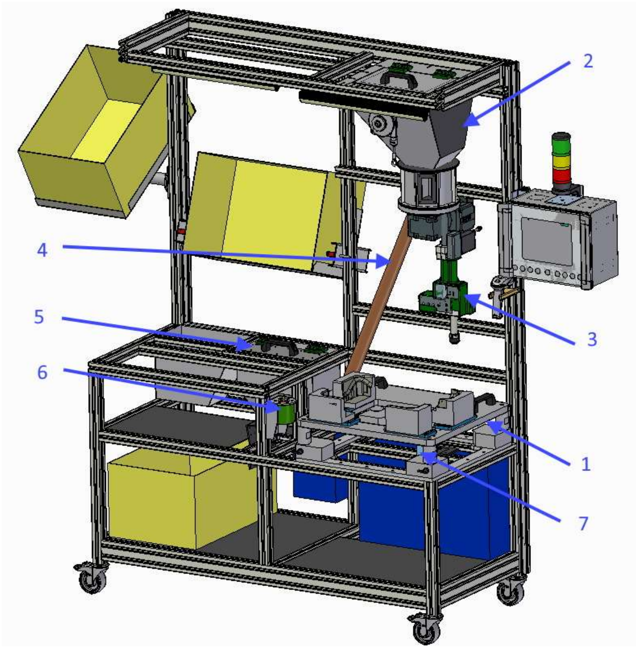

Fig. 5. View of an assembly station

The designed station is mobile thanks to transportation wheels. The frame of the station is made of aluminium profiles. The station has a changeable assembly nest (1), which makes it possible to assemble products of different geometries. Under the assembly nest there is a barcode scanner (7) for product identification and automatic setting of the number of released washers per one assembly cycle. The average height of the assembly table is 950 mm, which ensures ergonomic work conditions for the operator [7] (Fig. 6). The station also consists of a space for mat containers, an additional manual scanner for mats, and a pin (6) that allows the device to complete the washer release cycle in case of assembly error. The ergonomics of the workstation arrangement was checked based on the reach ranges presented in Fig. 7.

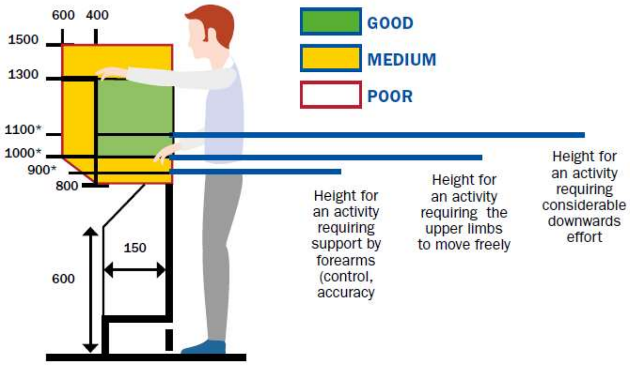

Fig. 6. Ergonomic windows for a standing workstation (side view)

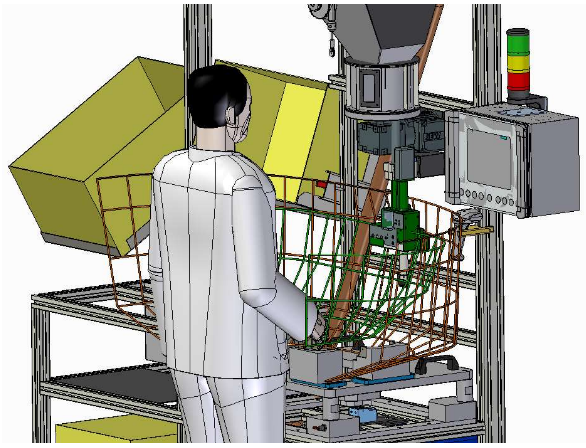

Fig. 7. Analysis of compliance with ergonomic conditions

Washers are fed into a feeder (5) and through a pipe (4) transported to a dispenser (2) by means of an air amplifier. The dispenser also includes an intake hopper with separating plates (Fig. 8) At the bottom of the hopper there is a dosing disc powered by a motoreducer. The disc has cut-out holes, thanks to which the washers are transported to the feed pipe which is closed with a valve (2) driven by a pneumatic actuator (3). A coupling (4) makes it possible to connect tools. The presence of a tool is signalled by a cased sensor which makes the valve open if the storage needs to be refilled.

The tool shown in Fig. 9 is hung up on a spring balancer in order to minimise the power that is necessary to move it. The tool has a 3D printed casing and a profiled clamp for the washer storage.

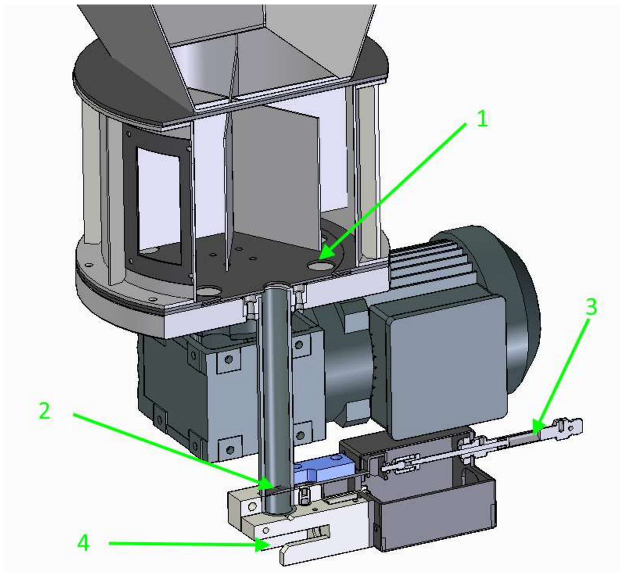

Fig. 8. Washer feeder

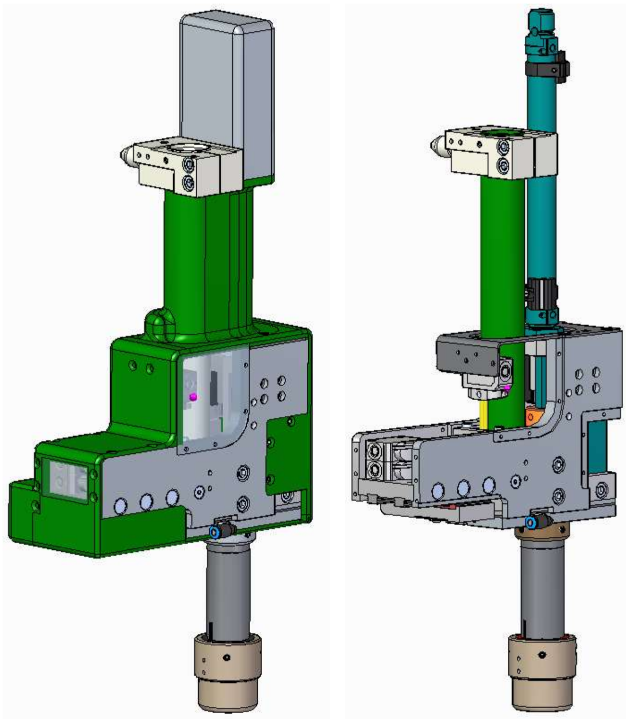

Fig. 9. View of an assembly tool

Fig. 10 illustrates the principle of tool operation. Washers are fed into the storage which is connected with the feeder. The minimum feed amount is controlled by a sensor (1). On launching the assembly readiness procedure, the tool is activated automatically. A slider (2) moves in direction A. As it is moving, a light gate confirms that the washer is in the slider hole. Once the washer is put under a pusher (3), the pusher is moved downwards (motion B) by an actuator (4). The washer is moved to the bottom of the head and supported on a bush necking (5). When the actuator (4) reaches the maximum position, the slider returns to the washer loading position (motion C). It should be noted that the position of the washer in the slider hole is maintained by negative pressure, which prevents washer displacement due to the action of external forces. When the operator puts the tool on a pin and sensors (6) detect the pin in the slider hole, the main assemble motion D is started – the motion is induced by an actuator (7). The washer is pushed out of the bush and assembled on the pin. When the operation is complete, the pusher returns to the initial position, and the entire cycle is repeated.

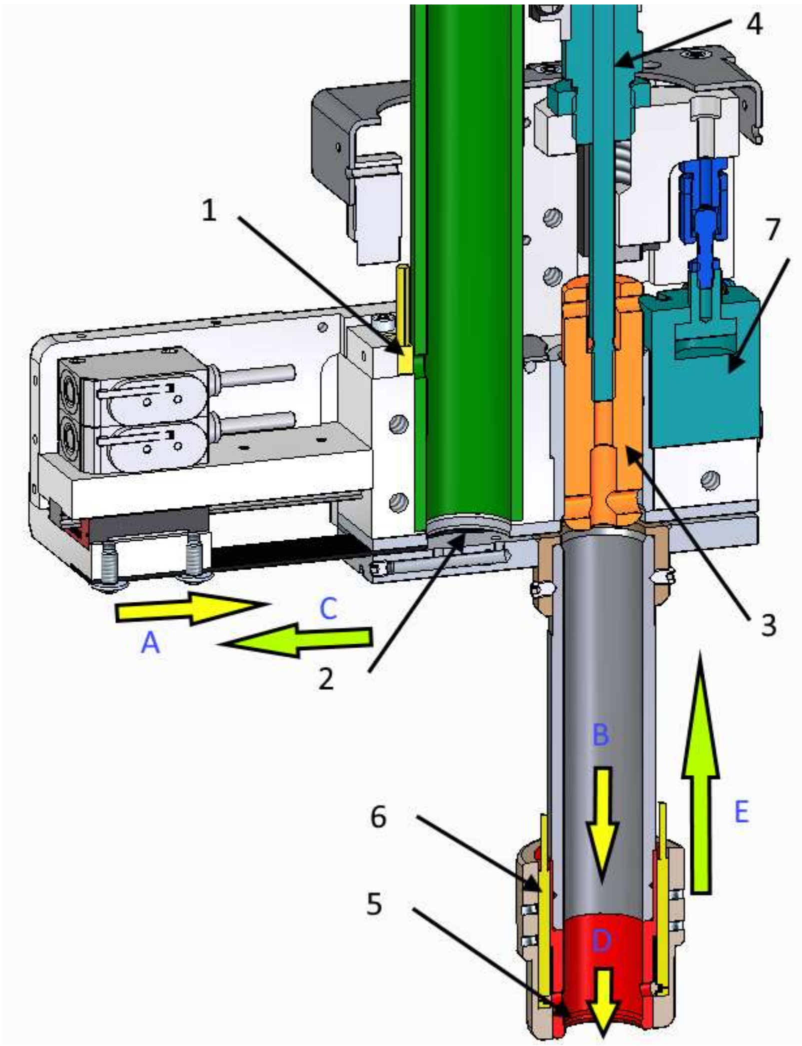

Fig. 10. Schematic diagram of tool design

4. Conclusion

The proposed design solution for the automated assembly of washers on ISO pins made it possible to meet the following requirements defined by the customer:

- automated assembly of washers,
- control of the number of released components,
- simple reconfiguration of the station to assemble products of different geometries,
- mobility of the station,
- ergonomic work conditions for the operator.

All the above-mentioned factors led to increased efficiency of the assembly process. The applied technological solutions ensured the repeatability of the process. The use of tools for product identification enabled automatic reversing of the machine to the required work conditions, which considerably reduced the probability of manufacturing a faulty product.

References

1. Domińczuk Jacek, 2018. „Analiza możliwości budowy wysokowydajnych elastycznych linii pakowania w oparciu o konstrukcje modułowe". *Technologia i Automatyzacja Montażu* 2 : 11-15.
2. Domińczuk Jacek, Kost Gabriel, Łebkowski Piotr, 2021. *Automatyzacja i robotyzacja procesów produkcyjnych*. Warszawa: Polskie Wydawnictwo Ekonomiczne.
3. Kluz Robert, 2012. „Projektowanie modułowego stanowiska montażowego". *Technologia I Automatyzacja Montażu* 1 : 9-13.
4. Kozioł Stanisław, Samborski Tomasz, Siczek Mariusz, Zbrowski Andrzej, 2018. „System for testing resistance for static exposure to dust". *Technologia i Automatyzacja Montażu* 2 : 11-15.
5. Kozioł Stanisław, Samborski Tomasz, Zbrowski Andrzej, 2021. „Design of an innovative window-to-balcony building module". *Technologia i Automatyzacja Montażu* 3 : 10-14.
6. Łunarski Jerzy. Redakcja: Sęp Jarosław. 2021. „Wprowadzenie". *Mechanika, Technika i technologia montażu maszyn* 83 : 5.
7. Nowacka Wiesława Ł., 2010. *Ergonomia i ergonomiczne projektowanie stanowisk pracy*. Warszawa: Wydawnictwo Politechniki Warszawskiej.

Marek Rośkowicz[1], Iga Barca[2]

DOI: 10.7862/tiam.2022.3.6

ANALYSIS OF THE AIRFRAME REPAIR NODE

ANALIZA WĘZŁA NAPRAWCZEGO POKRYCIA PŁATOWCA

Abstract

Polymer composite materials can be used both for the production of semi-monocoque structures and for the repair of aircraft airframes. Of all the elements of the semi-monocoque structure, the airframe skin is most often damaged during operation. The fragments of the skin between the frame elements of the semi-monocoque structure are considered as a thin-walled plate. The paper presents an analysis of the repair node of a metal plate subjected to uniform shear. The model of the repaired plate made in the Ansys Workbench environment was used for the analysis. The boundary conditions were defined by means of an articulated frame using the possibilities of the computing environment in the scope of, defining elements among others. The model was initially verified experimentally, assuming that it can be used to carry out a comparative analysis of two methods of repairing a damaged plate, using CFRP (Carbon Fiber Reinforced Polymer) and GFRP (Glass Fiber Reinforced Polymer) materials. Analyzing the obtained results, it was found that the repair does not restore the original strength of the damaged structure, however, it reduces the stress of the plate material around the opening by 10%.

Keywords: numerical analysis, experimental research, repair node, semi-monocoque structure, buckling, Ansys Workbench

Streszczenie

Polimerowe materiały kompozytowe mogą być wykorzystywane zarówno do wytwarzania elementów konstrukcji półskorupowych jak i do napraw już eksploatowanych metalowych płatowców statków powietrznych. Spośród wszystkich elementów konstrukcji półskorupowej, pokrycie płatowca ulega najczęściej uszkodzeniom eksploatacyjnym. Fragmenty pokrycia pomiędzy elementami szkieletu konstrukcji półskorupowej rozpatruje się jako płytę cienkościenną. W pracy przeprowadzono analizę węzła naprawczego metalowej płyty poddanej równomiernemu ścinaniu. Do analizy wykorzystano model naprawianej płyty wykonanej w środowisku Ansys Workbench. Warunki brzegowe zdefiniowano za pomocą przegubowej ramki wykorzystując możliwości środowiska obliczeniowego w zakresie m.in. definiowania kontaktów. Model wstępnie zweryfikowano eksperymentalnie, przyjmując założenie, że może być wykorzystywany do przeprowadzenia analizy porównawczej dwóch metod naprawy uszkodzonej płyty, z wykorzystaniem materiałów CFRP (Carbon Fibre Reinforced Plastic) oraz GFRP (Glass Fibre Reinforced Plastic). Analizując otrzymane wyniki stwierdzono, że naprawa nie przywraca pierwotnej wytrzymałości uszkodzonej struktury, jednakże zmniejsza wytężenie materiału płyty wokół otworu o 10%.

Słowa kluczowe: analiza numeryczna, badania doświadczalne, węzeł naprawczy, struktura półskorupowa, wyboczenie, Ansys Workbench

1. Introdution

The airframes of modern aircrafts are most often semi-monocoque structures [1], which consist of a frame and load-carrying skin [2]. Both the frame and the skin contribute to the load transmission. The share of airframe elements structure in the distribution of loads (bending and torsion) is unequal.

Normal stresses resulting from bending are transferred mainly by the wing spars, stringers and skin, while the shear stress resulting from bending and torsion are loaded by wing spars wall and skin. During the strength analysis, the skin is considered as a thin-walled plate [3]. One of the special features of each thin-walled structure is its low bending stiffness in the direction perpendicular to the skin plane and its susceptibility to loss of stability and buckling [4, 5].

In the process of operation, the airframe skin is the element that is most often damaged (98 - 100%) [6]. The damage may be a single element damage or a coupled damage (the skin and, additionally, other elements of the aircraft are damaged, e.g. stringers, wing spars, other force elements of the frame) [7,8,9]. These damages are particularly important when they occur in the wing structure, due to its tasks, including the creation of lift, stability and controllability [10]. Damage most often occurs as a result of impact on the structure, e.g. in conditions of improper use. In the case of a military aircraft, additional damage may occur due to the effect of combat measures [6, 11].

[1] dr hab. inż. Marek Rośkowicz, marek.roskowicz@wat.edu.pl, ORCID: 0000-0003-0501-0622.
[2] mgr inż. Iga Barca, iga.barca@wat.edu.pl, ORCID: 0000-0003-4687-4873.

In the process of maintenance, aircraft airframes are repaired. Repairs are carried out in order to restore the original strength of the structure and stop the process of damage development [12, 13]. In aviation, two basic methods of repairing aircraft skin are used: the method with the use of metal patches and mechanical joints [14] and the use of composite patches and adhesive joints [15, 16] or alternatively a hybrid solution [17, 18, 19]. Due to the technological susceptibility of fiber-reinforced composite materials, these types of materials are used to repair not only composite but also metal structures. Polymer composite materials are bonded to the damaged structure with adhesive materials [20, 21].

The purpose of the performed calculations and tests was to assess the effectiveness of repairing a damaged plate, which was subjected to uniform shear. The metal plate was repaired with composite materials. Implementation of works on experimental tests and calculations using the finite element method were performed. Using the finite element method, calculations were carried out on the basis of a metal plate model which was repaired with composite patches.

2. Model of plate and frame

In order to perform numerical calculations, a simplified model of the plate with a loading frame was prepared in the NX 11 environment. As part of the model being performed, the plate, repair elements, articulated joints and a frame for mapping the plate shear were defined. The following assumptions were adopted to define the plate model: thickness 1 mm and material properties of the 2024-T3 series aluminum alloy. The geometrical dimensions of the plate with a damage in the form of a hole with a diameter of 50 mm are presented in Fig. 1.

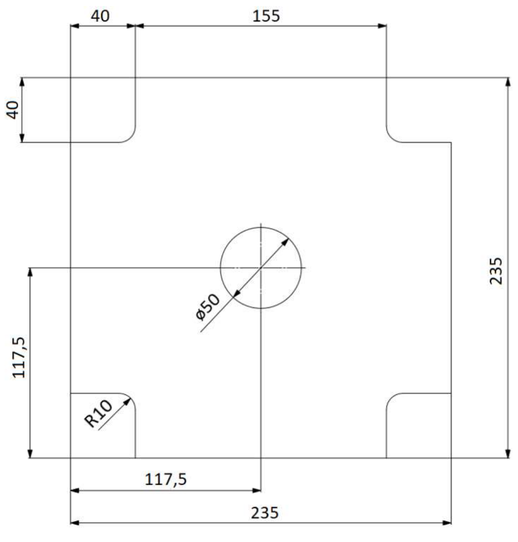

Fig. 1. Dimensions and shape of the plate used in the test

The model of the repaired plate consisted of elements that are used in the repair process. Inside the hole, a metal insert is defined, while on one of the outer surfaces of the plate a composite patch with the material properties of a glass (GFRP) and carbon (CFRP) composite was modeled. The properties of the glass composite corresponded to the material prepared on the basis of SynglassE86 glass fabric with a grammage of 101 g/m^2 and the L285/H285 (MGS) impregnated by Havel Composites (Fig. 2).

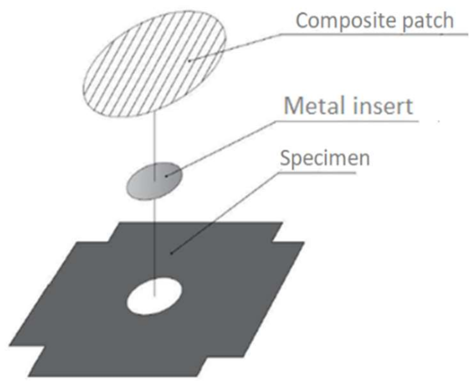

Fig. 2. Elements of the repair node

The properties of the carbon composite were defined on the basis of 160 g/m^2 carbon fabric by HACOTECH and L285/H285 (MGS) by Havel Composites. The composite patch had the shape of a clipped cone with a back diameter of 142 mm and a top layer diameter of 127 mm (Fig. 3). Due to the use of a conical shape, the occurrence of stress concentration in the joint of the adhesive joint at the edges of the edge overlap was limited. Between the patch and the panel to be repaired, an adhesive layer was modeled with a thickness of 0.1 mm, diameter of 142 mm and the properties of Epidian 57/Z1 adhesive [22].

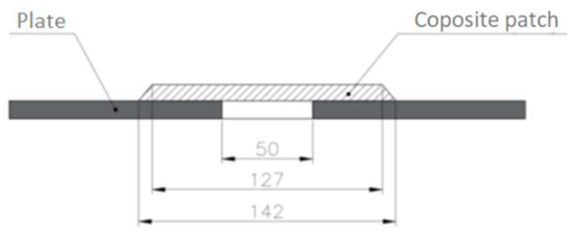

Fig. 3. The diagram of the repair node

As part of defining the boundary conditions in the load area, a model of the mounting frame was made, which consists of eight steel flat elements connected with each other articulated with four pivots. The scheme of the frame with the plate being repaired is shown in Fig. 4.

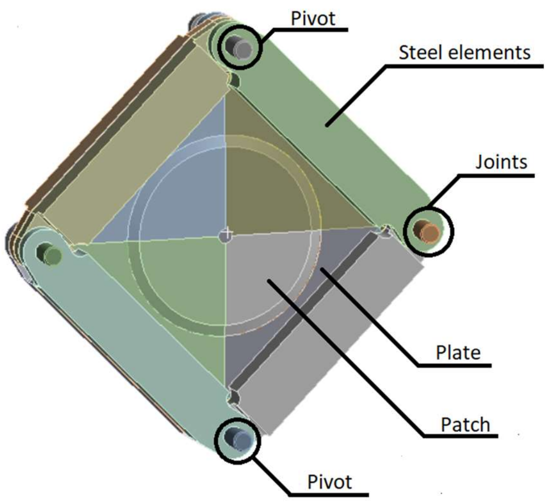

Fig. 4. Geometric model of the repaired plate with a frame

The plate geometries with the frame were exported to the Ansys Workbench 21 R2 environment for numerical calculations. For the preparation of the calculation model, the material properties of individual elements were defined. Epidian 57 adhesive parameters were adopted from the publication [22]. As part of solving the task, a simplification assuming quasi-isotropic properties of composite materials was adopted. Properties of the materials defined in the model are presented in Table 1.

Table 1. Properties of materials defined for calculations

Material	Young's module [MPa]	Poisson number
Aluminium alloy 2024-T3	73100	0,33
Adhesive Epidian 57/Z1	2083	0,35
Glass composite (GFRP)	40000	0,4
Carbon composite (CFRP)	61340	0,3
Steel elements - Steel	200000	0,3

Using the symmetrical layout of the plate, a regular shape of the plate mesh was defined. For this purpose, the board model was divided into 8 elements (Fig. 5). This type of operation was aimed at obtaining a mesh with a regular shape - Fig. 6.

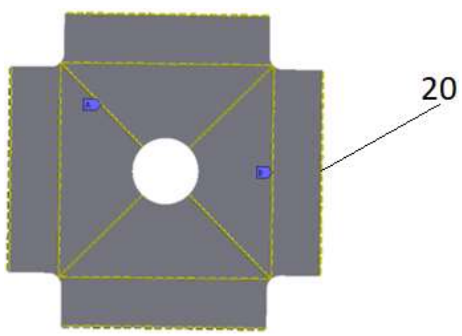

Fig. 5. Scheme of division of the slab model into 8 geometric elements

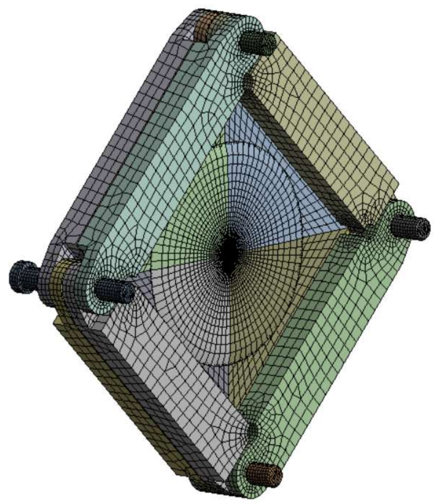

Fig. 6. The view of the model with the division into finite elements, the so-called mesh

The Edge Sizing option was used to define the mesh, assigning 20 elements to individual edges, and the MultiZone option, assuming the type of Hexa element. According to the adopted scheme, a similar division of the composite patch, the adhesive layer and the insert was made. Additionally, the frame elements have been assigned an optimization module of the Hex Dominant type. As a result of discretization, the frame model had 53362 finite elements and 62506 mesh nodes, while the repaired plate had 2400 elements and 5000 nodes.

3. Defining contact elements

In order to recreate the conditions of assembly the plate to the frame, bonded contacts have been defined between the frame and the plate. The same type of contact is defined between the composite patch and the adhesive layer and between the adhesive layer and the plate and between the insert and the adhesive layer. Figure 7 shows the individual elements for which the type of bonded contact has been defined.

The articulated joints were modeled between the frame elements and the pivots using a No Sepatarion contact (slip without friction, Fig. 8).

The last type of contact that was used in the modeling of the plate with the frame was the Frictional contact, which was assigned to the side surfaces of the insert and the hole. For the purposes of the analysis, the friction coefficient of 0.1 was assumed.

In the load area, a force of 8 kN was defined located in the pivot No. 1 directed along the z axis, while the pivot No. 4 was fixed using the Fixed Support function (Fig. 9).

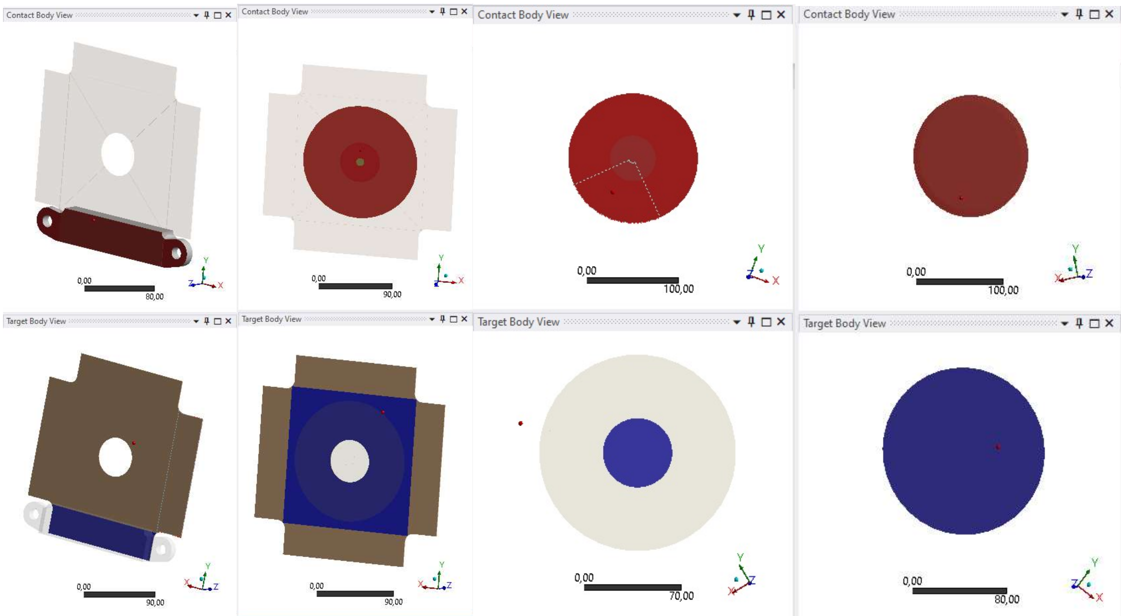

Fig. 7. Bonded contacts between the individual elements (red and purple indicate the contact area), from the left, the frame with the plate, the adhesive layer with the plate, the adhesive layer with the insert and the adhesive layer with the patch

Fig. 8. View of elements between which a No Separation type connection has been defined

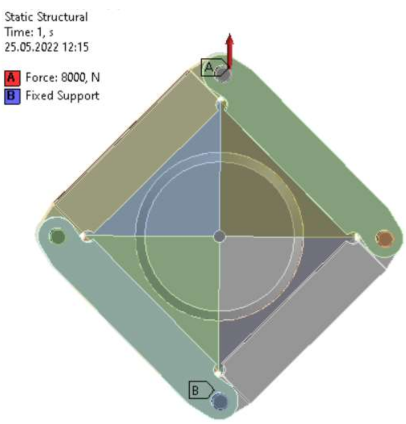

Fig. 9. The diagram of the boundary conditions of the FEM model

4. Experimental verification of the model

In order to made assess the quality of the model, calculations were carried out under the conditions of the planned experiment (8 kN load). The obtained results, in regard to of strain, were compared with the results of experimental tests.

4.1. Experimental tests of the plate

The specimen for experimental tests was made of 1 mm thick 2024-T3 sheet, aluminium alloy with the dimensions shown in Fig. 1. The repair of the plate consisted of installing a metal insert in a hole with a diameter of 50 mm. The composite patch was formed of 16 layers of SynglassE86 glass fabric with diameters from 127 mm to 142 mm, in 1 mm increments. The test surface was degreased with extraction naphtha and with the use of a 3M SC-DR disc of granularity P180 and P400. Only the area on which the patch was to be formed was processed. The surface preparation process was completed with another surface cleaning with extraction naphta. The L285 epoxy resin mixed with the H285 hardener in the proportions 100: 40 was used as the saturant of the composite patch. The filtered material layers were layered according to the scheme [0°, 30°, 60°, 90°]4. Then, next layers used in the vacuum bag technology, including a resin draining mat, perforated foil and delaminating fabric, were applied to the composite patch. The patch prepared in this way was placed in a device enabling to generate a pressure equivalent to a pressure of 0.8 MPa and left for 24 h at room temperature (according to the technical sheet for curing resin L285/H285). The prepared composite patch was adhesively bonded to the plate with the use of Epidian 57 epoxy resin mixed with the hardener Z1, in a ratio of 1:10. The adhesive has been hardened: in the first stage, 24 hours at 20°C and for 6 hours at 80°C.

After the specimen was prepared, mounting holes were drilled in it and the specimen with the frame was placed in the traverses of the testing machine. The specimen and the method of its mounting in the machine are shown in fig. 10.

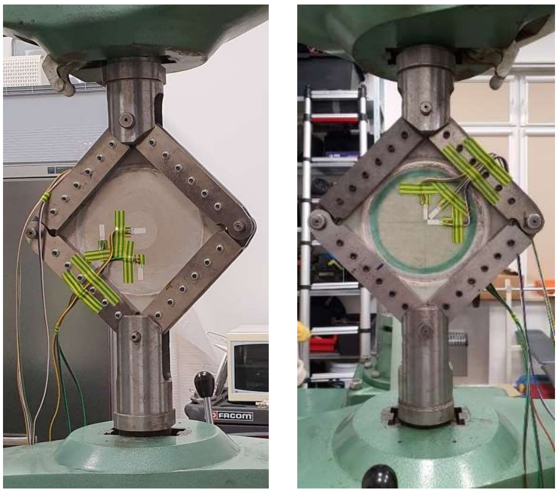

Fig. 10. Fixing the sample in the testing machine

Strain gauges were jointed to the elements of the repair node in accordance with the diagram shown in Fig. 11.

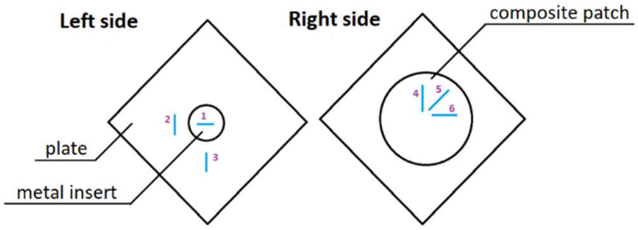

Fig. 11. Distribution and numbering of strain gauges mounted on the specimen

The strain gauge No. 1 is jointed to the metal insert - in the direction perpendicular to the load generated by the testing machine. Strain gauges 2 and 3 were jointed in the direction of load deformation of the testing machine. The strain gauges 4, 5, 6 had the form of a rosette bonded to the composite patch. A CL 460 (Zakład Elektroniki Pomiarowej Wielkości Nieelektrycznych, Poland) bridge was used to measure the deformation.

The results of the recorded strain from the experimental tests were compared with the results of the numerical simulation (Fig. 12 and Table 2).

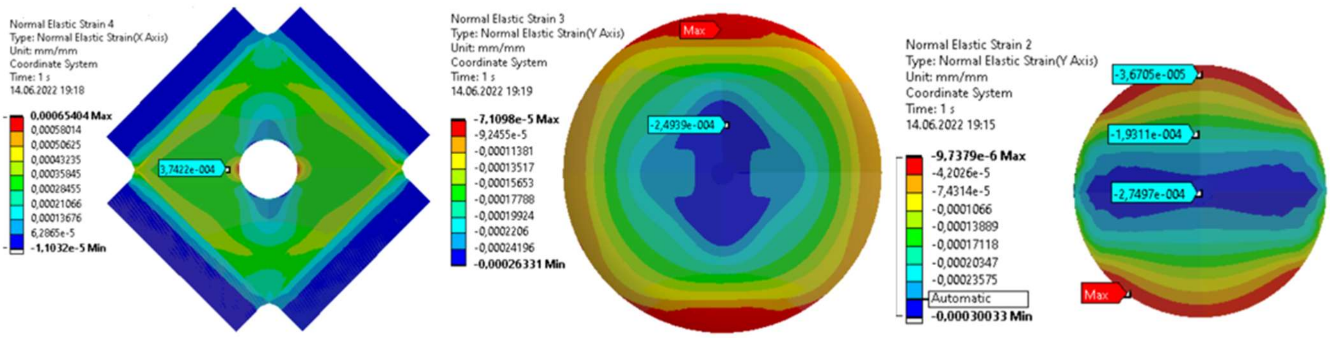

Fig. 12. Deformation values for the plate, glass fiber patch and reinforcement insert

Table 2. Values of deformations obtained in the experimental test and numerical simulation

	Canal 1	Canal 2	Canal 3	Canal 4	Canal 5	Canal 6
	m/m	m/m	m/m	m/m	m/m	m/m
Experiment	-0,000465	0,000685	0,000598	0,00098	-0,000081	-0,000545
Calculations	-0,000300	0,000654	0,000654	0,00035	-0,000050	-0,000260

The largest differences in strain between the results of the experimental tests and the results of calculations occur on the composite patch, which may be related to the take simplifications in defining the composite material. In the case of strain gauges bonded directly to a metal plate, the differences are at the level of several percent. Therefore, it was assumed that the prepared model can be used for further analyzes.

5. Calculations of the repairing plate

In order to compare the effectiveness of the plate repair with different composite materials (CFRP and GFRP), calculations were carried out using the prepared model. Under boundary conditions, the load values were changed from 8 kN to 25 kN. According to the results presented in [23], it was the range of subcritical loads in buckling process of plate. Computational simulations were carried out for the undamaged, damaged and repaired plate model. Examples of calculation results in the form of reduced stresses (von-Mises) for an undamaged and damaged plate are presented in Fig. 13.

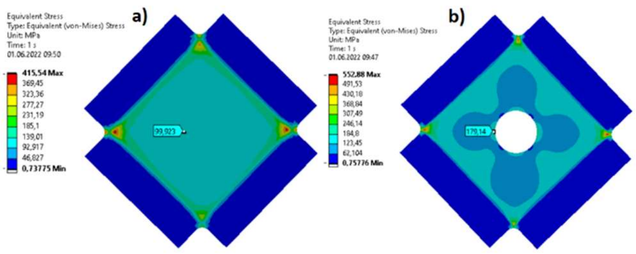

Fig. 13. Reduced stresses in the plate for undamaged (a) and damaged (b)

Stress concentration in an undamaged plate occurs near the corners of the plate. Which in the conditions of a semi-monocoque structure may cause additional stress on the mechanical joints. In the central zone of the plate, where the stress wave formation process takes place, the stress values are below the yield point. Figure 14 presents the results of the stress distribution in the plate repaired with composite patch in two variants (option I - glass composite GFRP, option II - carbon composite CFRP).

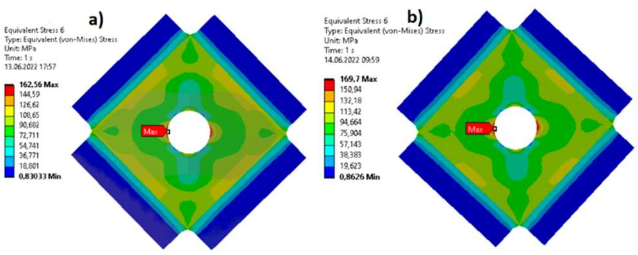

Fig. 14. Reduced stresses in the plate with the GFRP (a) and CFRP (b) patch

Using both GFRP and CFRP, the effort conditions of the undamaged plate were recreated. The greatest changes were observed in the area of the insert mounting hole. The comparison of normal stresses perpendicular to the adhesive surface and the maximum main stresses in the adhesive layer for two patch variants is shown in Fig. 15 and Fig. 16.

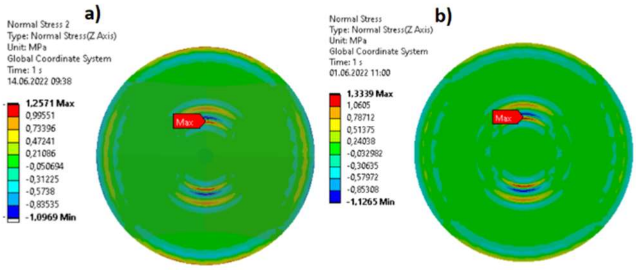

Fig. 15. Normal stresses to the adhesive surface for two patch variants: GFRP (a), CFRP (b)

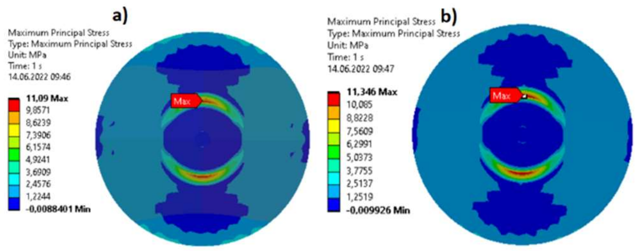

Fig. 16. Maximum main stresses in the adhesive layer for two patch variants: GFRP (a), CFRP (b)

The values of stresses in the adhesive joint area are lower than the values of breaking stresses defined for Epidian 57/Z2. Table 3 presents the displacement values of the frame model with the specimen for the considered repair values. The smallest values occurred for the CFRP composite patch.

Table 3. Displacement values of the frame with the plate for the considered cases

The type of the plate	Plate without damage	Plate with damage	Plate – glass patch	Plate – carbon patch
Displacement in the direction of the load [mm]	0,38	0,43	0,248	0,25

6. Conclusions

Based on the calculations and experimental tests performed, the following conclusions can be defined:

- the aircraft skin repair node, in which composite materials are used, can locally "stiffen" a part of the semi-monocoque structure. The consequence of repairing the skin located between the frame elements of the semi-monocoque structure may be a greater effort of the mechanical joints located in the vicinity of the repaired area.
- repair does not restore the original strength of the damaged structure, however, it reduces the strain of the plate material around the opening by about 10%.
- regardless of the taken variant of the composite patch (GFRP, CFRP), the effectiveness of the repair should be confirmed in experimental tests (especially with the use of the CFRP patch - low susceptibility to deformation of carbon fibers in the process of plate buckling may cause an unfavorable phenomenon of peeling off of the composite patch.
- it seems that in order to evaluate the adopted solutions more effectively, the composite patch for calculations should be defined as layered materials - (the homogenization of the material properties of the composite patch adopted for calculations may negatively affect the stress distribution in the adhesive layer.

Bibliography

1. Beukers A., Bersee H., Koussios S., Future "Aircraft Structures: From Metal to Composite Structures". Springer. 2011.
2. Standridge Michael., "Aerospace materials — past, present, and future". Aerospace Manufacturing and Design. 2014.
3. Cichosz Edmund, Kierkowski Jerzy, „Przybliżone obliczenia wytrzymałościowe płatowca". WAT. Warszawa 1968.
4. Bałon P., Świątoniowski A., Rejman E., Kiełbasa B., Smusz R., Szostak J., Kowalski Ł., Bałon N., Cieślik J., „Zastosowanie cienkościennych konstrukcji integralnych w lotnictwie na przykładzie SAT-AM". Zeszyty naukowe Politechniki Rzeszowskiej 300, Mechanika 92 RUTMech, t. XXXVII, z. 92 (2020), s. 5-17.
5. Zerbst U., Heinimann M., Donne C.D., Steglich D., "Fracture and damage mechanics modelling of thin-walled structures – An overview". Engineering Fracture Mechanics 76 (2009) 5-43.
6. Godzimirski J., „Naprawa płatowców". WAW. Warszawa 1998.
7. Tavares S.M.O., de Castro P.M.S.T., "An overview of fatigue in aircraft structures". Fatigue & Fracture of Engineering Materials & Structures. 2017.
8. Jones A., Peel C.J., "The analysis of aircraft component failures". In: Goel V.S. editor. Analysing failures: the problems and the solutions. Cleveland, OH: American Society for Metals, 1986.
9. Jones R., Chiu W.K., Smith R., "Airworthiness of composite repairs: failure mechanisms". Engineering Failure Analysis. 1995: 2: 117-128.
10. Galiński C., „Wybrane zagadnienia projektowania samolotów". Biblioteka Instytutu Lotnictwa, Warszawa 2016.
11. Lewitowicz J., „Podstawy eksploatacji statków powietrznych, cz. 4". Wydawnictwo ITWL, Warszawa 2007.
12. Goranson Ulf G., "Fatigue issues in aircraft maintenance and repairs". Elsevier. Boeing Commercial Airplane Group, Seattle, WA, USA. 2017.
13. Bouiadjra B.B., Benyahia F., Albedah A., Bouiadjra B.A.B., "Comparison between composite and metallic patches for repairing aircraft structures of aluminium alloy 7075 T6". International Journal of Fatigue 80 (2015), 128-135.
14. Kedward K., Kim H., "Joining and Repair of Composite Structures". ASTM Stock Number: STP1455, International, USA, 2005.
15. Katnam K.B., Da Silva L.F.M., Young T.M., "Bonded repair of composite aircraft structures: A review of scientific challenges and opportunities". Progress in Aerospace Sciences 61 (2013) 26-42.
16. Baker A., Chalkley P., "Development of a generic repair joint for certification of bonded composite repairs". International Journal of Adhesion and Adhesives, vol. 19, 1999.
17. Romilly D.P., Clark R.J., "Elastic analysis of hybrid bonded joints and bonded composite repairs". Composite Structures Volume 82, Issue 4, 2008, Pages 563-576.
18. Chang P., Heller M., Wang J., Opie M., Yu X., "A New Approach for Hybrid Bonded Repair of Metallic Components" Journal article in preparation, 2017.
19. Wang J., Baker A., Chang P., "Hybrid approaches for aircraft primary structure repairs" Composite Structures, 2018.
20. Chester R., Chapter 2 Materials Selection and Engineering. "Advances on the Bonded Composite Rapair of Metallic Aircraft Structure", vol. 1, pp. 19-40. Australia 2002.
21. Baker A., Chester R., Mazza J., "Bonded Repair Technology for Aging Aircraft". Defence Technical Information Center, Compilation Part Notice ADP014082. 2001.
22. Godzimirski J., Tkaczuk S., "Numerical calculations of adhesive joints subjected to shearing". Journal of Theoretical and Applied Mechanics. 45, 2 pp. 311-324, Warsaw 2007.
23. Rośkowicz M., Tkaczuk S., „Połączenia adhezyjne w naprawach pokryć płatowców". Technologia i Automatyzacja Montażu. 3/2010, pp. 32-35.

This work was financed by Military University of Technology under research project UGB 779/2022.